

Re-Evaluating the Mechanism of Action of α,β -Unsaturated Carbonyl DUB Inhibitors B-AP15 and VLX1570: A Paradigmatic Example of Unspecific Protein Crosslinking with Michael Acceptor Motif-Containing Drugs

Jennifer Ward, Adán Pinto-Fernández, Loïc Cornelissen, Sarah Bonham, Laura Diaz Saez, Olivier Riant, Kilian Huber, Benedikt M. Kessler, Olivier Feron, Edward W. Tate

Submitted date: 23/10/2019 • Posted date: 25/10/2019

Licence: CC BY-NC-ND 4.0

Citation information: Ward, Jennifer; Pinto-Fernández, Adán; Cornelissen, Loïc; Bonham, Sarah; Saez, Laura Diaz; Riant, Olivier; et al. (2019): Re-Evaluating the Mechanism of Action of α,β -Unsaturated Carbonyl DUB Inhibitors B-AP15 and VLX1570: A Paradigmatic Example of Unspecific Protein Crosslinking with Michael Acceptor Motif-Containing Drugs. ChemRxiv. Preprint.

Deubiquitinating enzymes are a growing target class across multiple disease states, with several inhibitors now reported. b-AP15 and VLX1570 are two structurally related USP14/UCH-37 inhibitors with a shared α,β -unsaturated carbonyl substructure motif. Initially taken forward into a phase I/II clinical trial for refractory multiple myeloma, VLX1570 has since been put on full clinical hold due to dose limiting toxicity. Through a proteomic approach, here we demonstrate that these compounds target a diverse range of proteins, resulting in the formation of higher molecular weight complexes. Activity-based proteome profiling identified CIAPIN1 as a sub-micromolar covalent target of VLX1570, and further analysis demonstrated that high molecular weight complex formation leads to aggregation of CIAPIN1 in intact cells. Our results suggest that in addition to DUB inhibition, these compounds induce non-specific protein aggregation through cross-linking, providing a molecular explanation for general cellular toxicity.

File list (4)

VLX_Manuscript_Submission.pdf (885.02 KiB)	view on ChemRxiv • download file
VLX_Manuscript_Submission.docx (479.54 KiB)	view on ChemRxiv • download file
VLX_Supporting information_Submission.pdf (1.24 MiB)	view on ChemRxiv • download file
Supporting Dataset 1.xlsx (110.48 KiB)	view on ChemRxiv • download file

Re-evaluating the mechanism of action of α,β -unsaturated carbonyl DUB inhibitors b-AP15 and VLX1570: a paradigmatic example of unspecific protein crosslinking with Michael acceptor motif-containing drugs.

Jennifer A. Ward,^{1,2,5*} Adan Pinto-Fernandez,^{2,4*} Loïc Cornelissen,³ Sarah Bonham,² Laura Díaz-Sáez,^{1,2} Olivier Riant,⁴ Kilian V. M. Huber,^{1,2} Benedikt M. Kessler,² Olivier Feron,³ and Edward W. Tate⁵

¹Structural Genomics Consortium, Nuffield Department of Medicine, University of Oxford, Oxford, UK.

²Target Discovery Institute, Nuffield Department of Medicine, University of Oxford, Oxford, UK.

³Institute of Condensed Matter and Nanosciences Molecules, Solids and Reactivity (IMCN/MOST), UCLouvain, Brussels, Belgium.

⁴Pole of Pharmacology and Therapeutics (FATH), Institut de Recherche Expérimentale et Clinique (IREC), UCLouvain, Brussels, Belgium.

⁵Department of Chemistry, Imperial College London, Molecular Sciences Research Hub, White City Campus, London, UK.

*Corresponding authors: jennifer.ward@ndm.ox.ac.uk and adan.pintofernandez@ndm.ox.ac.uk

Abstract

Deubiquitinating enzymes are a growing target class across multiple disease states, with several inhibitors now reported. b-AP15 and VLX1570 are two structurally related USP14/UCH-37 inhibitors with a shared α,β -unsaturated carbonyl substructure motif. Initially taken forward into a phase I/II clinical trial for refractory multiple myeloma, VLX1570 has since been put on full clinical hold due to dose limiting toxicity. Through a proteomic approach, here we demonstrate that these compounds target a diverse range of proteins, resulting in the formation of higher molecular weight complexes. Activity-based proteome profiling identified CIAPIN1 as a sub-micromolar covalent target of VLX1570, and further analysis demonstrated that high molecular weight complex formation leads to aggregation of CIAPIN1 in intact cells. Our results suggest that in addition to DUB inhibition, these compounds induce non-specific protein aggregation through cross-linking, providing a molecular explanation for general cellular toxicity.

Main

Ubiquitination, the covalent addition of the 76 amino acid protein ubiquitin (Ub) to protein substrates, is a widespread protein post-translational modification (PTM) in eukaryotic cells.¹ Due to its role in proteasomal degradation and a plethora of signalling pathways, ubiquitination is an emerging field of clinical interest in multiple

disease states, including cancer.²⁻⁴ Several compounds have been reported in recent years targeting deubiquitinating enzymes (DUBs)^{4, 5} which regulate the removal of Ub marks. However, the characterisation of such inhibitors and clinical compounds from a target perspective is variable; though a DUB target is reported, compound selectivity and specificity across the proteome remained in most cases incompletely resolved. Comprehensive understanding of a compound's targets facilitates interpretation of phenotypes in pre-clinical investigations, and can identify mechanisms of toxicity⁶ and resistance at an early stage of testing. Only recently, and with the help of advanced activity-based protein profiling (ABPP)⁷⁻⁹ assays that allow the profiling of DUBs in a cellular context, highly selective DUB inhibitors have been reported.^{4, 5, 10} Here, we describe the proteomic investigation of two structurally related DUB inhibitors b-AP15 and VLX1570. We demonstrate that these inhibitors target a diverse range of proteins, resulting in the formation of higher molecular weight (MW) complexes. Through a quantitative chemical proteomic approach, we identify CIAPIN1, also known as anamorsin, as a potent covalent target of VLX1570 which upon reaction with VLX1570 forms high molecular weight complexes leading to aggregation of CIAPIN1 in intact cells.

b-AP15 has been previously described as a specific reversible inhibitor of the proteasomal DUBs USP14 and UCH-37 (also referred to as UCH-L5) with anti-cancer activities.^{11, 12} Examination of the chemical structure of b-AP15, however, shows the presence of Michael acceptor motifs (**Figure 1A**) that are capable of covalent interaction with nucleophilic residues. Although the results obtained by D'Arcy and colleagues demonstrate that b-AP15 is an inhibitor of USP14/UCH-37,¹¹ two unrelated cysteine protease enzymes from different DUB families, its structure suggests additional proteins may be targeted by this compound class. Indeed, b-AP15 possesses higher potency in intact cells than in biophysical assays against USP14 and UCH-37.¹¹ In support of compound promiscuity, another study describing the chemical synthesis of active-site-directed DUB probes showed data compatible with a non-specific DUB inhibition profile upon increasing concentrations of b-AP15.¹³ In our hands, b-AP15 inhibits the cleavage of the DUB substrate Ub-AML (ubiquitin-aminoluciferin) by a number of purified recombinant DUBs (**Figure 1B**). Crude extracts of cells treated with increasing concentrations of b-AP15 also

showed that b-AP15 is able to decrease the global DUB activity of these treated cells (**Figure 1C**). Further, b-AP15 treatment in both cancer cell lines and endothelial cells resulted in comparable cytotoxicity as observed by a cell viability assay, indicating the non-specific toxicity of this chemotype (**Supplementary Figure 1**).

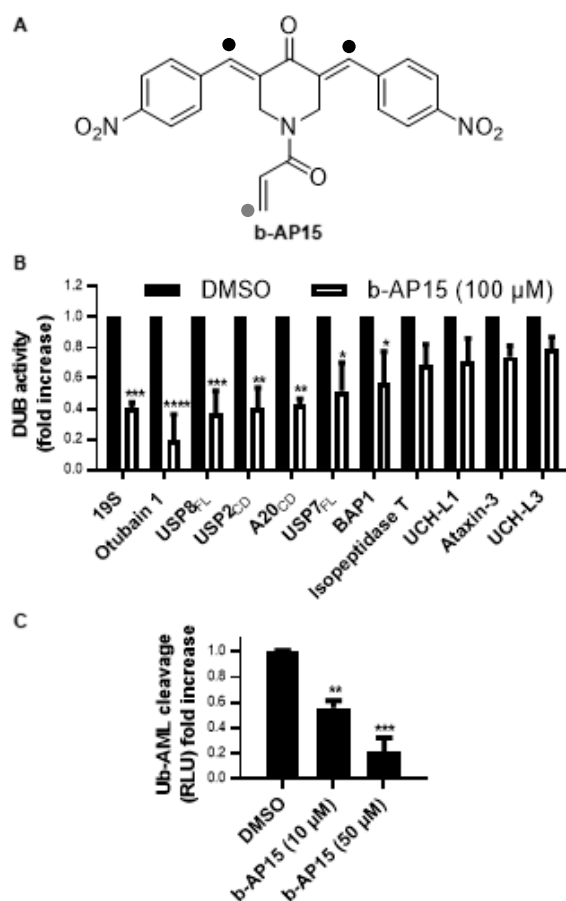


Figure 1. b-AP15 is a non-specific deubiquitinating enzyme (DUB) inhibitor. (A) Molecular structure of b-AP15 with Michael acceptors (black dot) and acrylamide (grey dot) motif indicated. (B) DUB activity measured by cleavage of the luminescent substrate Ub-AML in a panel of recombinant proteasomal (purified 19S proteasomes) and non-proteasomal DUBs treated with b-AP15 (100 μM) (n=3-4). (C) DUB assay as described above using HeLa cell extracts (5 μg) incubated with the indicated b-AP15 concentrations (n=3).

By immunoblot analysis, it was observed that b-AP15 induces the formation of high MW complexes with USP14 (**Figure 2A and 2B**) and UCH-37 (**Supplementary Figure 2**) in both crude cell extracts and intact cells. The formation of these complexes is reduced by co-incubation with thiol containing reducing reagents DTT or GSH, in support of these higher MW complexes forming via the Michael acceptors. The protective effect of these reagents was hypothesized to be due to the blocking of these reactive sites. To test this, b-AP15 was reacted *in vitro* with an

excess of GSH in PBS, representing conditions similar to those used in our *in vitro* and *in situ* assays. As predicted, b-AP15(GSH)₂ could be observed by LC-MS analysis after 1 hour of incubation. (**Supplementary Figure 3**). In support of this finding, PYR-41, an ubiquitin-activating enzyme (E1) inhibitor (also containing Michael acceptors), has been reported to induce DTT-sensitive protein cross-linking and inhibition of DUBs and other cellular enzymes by formation of high MW complexes¹⁴. In addition, high MW ubiquitylated proteins accumulated upon b-AP15 treatment, the levels of which were reduced by co-treatment with DTT and GSH (**Figure 2C**). The origin of these very high molecular weight ubiquitylated proteins that accumulate upon treatment with b-AP15 in comparison with those that accumulate on application of proteasome inhibitors has been largely discussed.^{11, 15} Interestingly, ubiquitylated protein complexes with very high MW are also reported by D'Arcy and other studies using α,β unsaturated carbonyl compounds.^{14, 16-18} The effects of b-AP15 on the global proteome were further evaluated by SDS-PAGE followed by Coomassie Blue staining, revealing the formation of notably increased levels of high MW protein complexes in comparison to DMSO control or co-treatment with DTT and GSH (**Figure 2D**). To better characterize the consequences of the global formation of high MW protein complexes on cell signalling, the status of mTOR was analysed in crude extracts treated with b-AP15 by immunoblotting. Strikingly, a shift from mTOR in its native form towards a band with slower migration mobility is observed with nanomolar concentration of bAP-15 (**Supplementary Figure 4A and 4B**). A similar observation was described by us in a previous study showing oxidation of proteins by a photosensitiser.¹⁹ A similar but less potent effect was observed on incubation with the natural product curcumin, which also possesses Michael acceptor groups (**Supplementary Figure 4C and 4D**).

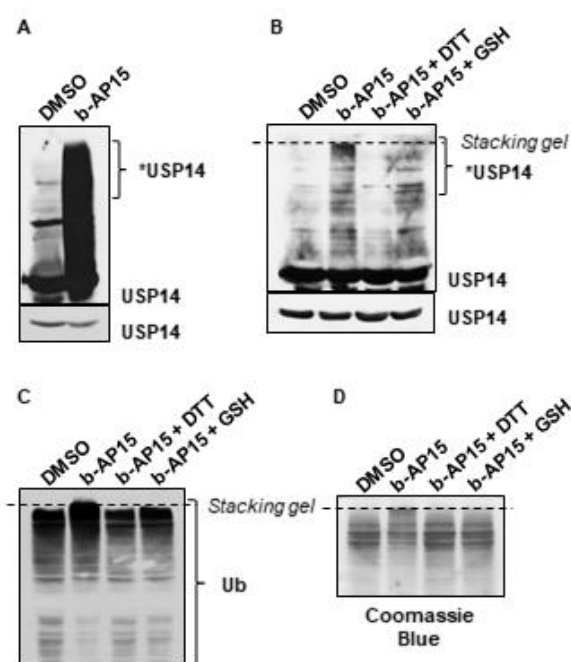


Figure 2. b-AP15 inhibits DUBs through the formation of cytotoxic high MW protein complexes, which are averted in the presence of thiol reducing agents. Immunoblot analysis of high MW complexes of USP14 in (A) HeLa crude cell extracts incubated with b-AP15 (10 μ M) and in (B) HeLa cells treated with either vehicle, 10 μ M b-AP15 or with 10 μ M b-AP15 in combination with reducing agents (10 mM dithiothreitol (DTT) or 10 mM glutathione (GSH)), both at 37°C for 2 hours. Shorter exposure times were used as a loading control (lower blots in the panel). (C) Immunoblot analysis of ubiquitin conjugates in HeLa cells treated with vehicle, 10 μ M b-AP15, or with 10 μ M b-AP15 in combination with reducing agents (10 mM dithiothreitol (DTT) or 10 mM glutathione (GSH)) for 2 hours. (D) Visualization of the b-AP15-induced high MW protein complexes in a SDS-PAGE gel, after Coomassie Blue staining, in HeLa cells treated as in (C).

VLX1570 is a structural analogue of b-AP-15 that shows higher potency and improved permeability.^{20, 21} VLX1570 was taken forward into a phase I/II clinical trial for refractory multiple myeloma in combination with dexamethasone (NCT02372240), but was then put on full clinical hold in July 2017 due to dose limiting toxicity. Based on our analysis of b-AP15, we postulated that this toxicity may be due to promiscuous covalent reaction with cellular nucleophiles and formation of high MW complexes. To test whether VLX1570 also forms high MW complexes, HeLa lysates were treated with varying concentrations of b-AP15 and VLX1570 and probed with the active-site-directed DUB probe HA-Ub-C2Br.²² Dose-dependent inhibition of probe labelling was observed for both compounds. Even on blotting for USP28, a DUB structurally unrelated to both USP14 and UCH-37, higher MW complex formation was observed (**Supplementary Figure 5**). Co-incubation of both VLX1570 and b-AP15 with GSH in the multiple myeloma cell line KMS11 led to increased cell

viability after 16 hours, suggesting that the GSH is scavenging these compounds and reducing their active concentration (**Supplementary Figure 6**).

GSH represents one of many nucleophiles accessible to VLX1570 within a biological context, and Michael acceptors are well known for their reactivity with cysteine residues.²³ To comprehensively profile the covalent targets of VLX1570, ABPP was conducted. Accordingly, an alkyne tagged analogue of VLX1570, Compound **1** (**Figure 3A**) was designed and synthesized. The acrylamide position was selected for conversion to the alkyne, as acrylamide-lacking analogues had previously been reported in structure-activity relationship studies not to influence cell viability.²⁰ Indeed, **1** retained equivalent cytotoxicity to VLX1570 in both KMS11 and U2OS cell lines, as observed with the CellTiter Glo assay (**Figure 3A, Supplementary Figure 7**).

Before commencing proteomic-profiling experiments, suitable competitive conditions were determined. U2OS cells were pre-incubated with increasing concentrations of VLX1570 or bAP-15 for 30 minutes before addition of the affinity probe **1** at a final concentration of 5 μ M. After 1 hour, the cells were lysed. Subsequent ligation to AzTB,²⁴ an azido-TAMRA-biotin capture reagent, via a copper catalyzed azide-alkyne cycloaddition (CuAAC) allowed visualization of probe-protein complexes by in-gel fluorescence. Both VLX1570 and b-AP15 pre-incubation caused a reduction in labelling intensity for specific bands, most markedly affecting a band at approximately 37 kDa (**Supplementary Figure 8A**). 5 and 20 μ M VLX1570 competitive conditions were taken forward for proteomic analysis. Spike-in SILAC methodology²⁵ was employed as previously described.^{8, 26} Briefly, cell lysates from competitive conditions were mixed in a 2:1 ratio with 'spike': lysate generated from **1**-treated U2OS cells grown in R10K8 media. Subsequent CuAAC ligation, enrichment on NeutrAvidin-Agarose resin, tryptic digest and LC-MS/MS analysis enabled proteome-wide in-cell target identification of **1**-labelled proteins. Multiple covalent targets were identified using this method, with significant competition observed at both 1- and 4-fold competitor excess. 44 proteins were significantly competed by 20 μ M VLX1570 (**Figure 3B, Supporting Dataset 1**), 24 of which were also significantly competed by 5 μ M of compound (**Supplementary Figure 8B**). On inspection of these protein sequences, all contained cysteine residues. Gene Ontology cellular component analysis suggested that VLX1570 was covalently interacting with proteins across multiple cellular locations, including the cytoplasm,

nucleus, and multiple organelles (**Supplementary Table 1**). It should be noted that although we have demonstrated accumulation of higher MW bands for UCH-37, USP14 and USP28 by immunoblot analysis, none of these DUBs were identified in the ABPP experiment. As the ABPP experiment only identifies covalent interactors, it is possible that the high MW complex formation observed for DUBs is occurring through a non-covalent mechanism. This is in agreement with literature data reporting that although DTT does affect cytotoxicity of VLX1570²⁰, compound binding and enzymatic inhibition are both reversible.²¹ Alternatively, it is possible that the high MW complexes formed with these proteins sterically hinder the CuAAC ligation reaction, thereby preventing covalently **1**-labelled proteins from being enriched and identified in this experiment.

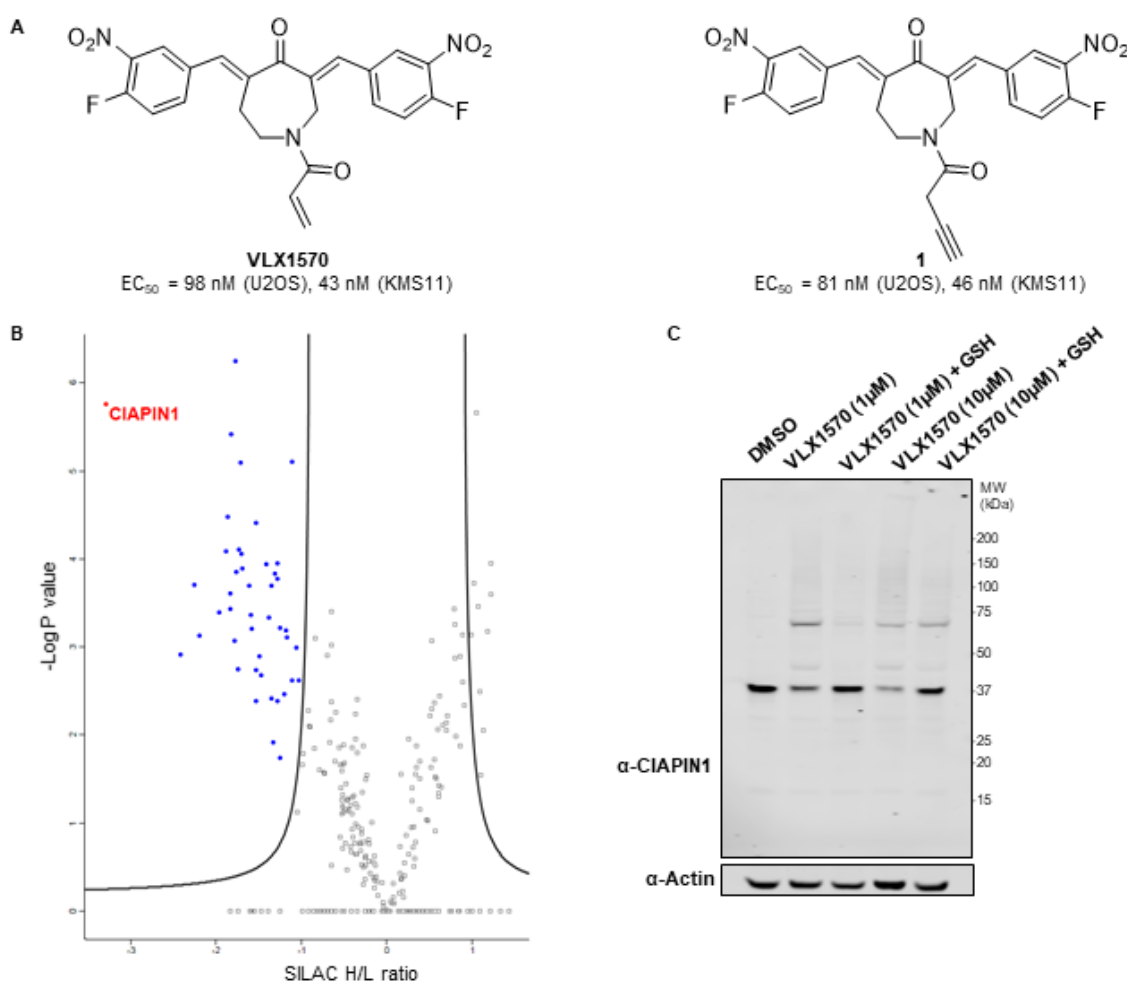


Figure 3. Chemical proteomics reveals multiple covalent targets of VLX1570. (A) Structure of VLX1570 and probe derivative compound **1**. EC₅₀ values measured by CellTiter Glo in U2OS and KMS11 cells are reported. (B) Volcano plot of **1**-enriched proteome from U2OS cells, with targets significantly (FDR=0.05, S0 = 0.2) competed by 20 μM VLX1570 indicated (blue). The most significant

hit, CIAPIN1, is indicated. **(C)** Immunoblot analysis of VLX1570 treated KMS11 cells demonstrates a protective effect against high MW complex formation for CIAPIN1 on addition of GSH (10 mM, 2 hr).

The most significantly competed covalent target of VLX1570 identified was CIAPIN1. CIAPIN1, a 33 kDa protein, is a part of the electron transport chain that enables Fe-S cluster assembly.²⁷ It possesses an N-methyltransferase domain at its N-terminus, though this has been reported to be catalytically inactive.²⁸ Further, CIAPIN1 exerts anti-apoptotic effects in cells though it is unrelated to apoptosis regulatory molecules of the BCL2 or CASP families.²⁹ In our hands, siRNA knockdown of CIAPIN1 lead to a reduction in cell viability of KMS11 cells (**Supplementary Figure 9**). Knockdown of CIAPIN1 has been reported to induce apoptosis in several cancer^{30, 31} and also non-cancer cell lines.^{32, 33} In agreement with functional inhibition of CIAPIN1, both b-AP15 and VLX1570 are reported to exert cytotoxicity via an apoptotic mechanism that is insensitive to BCL2 overexpression.^{11, 21}

As observed for DUB targets of this chemotype, higher MW complex formation was observed on immunoblotting for CIAPIN1 in VLX1570 treated cells, an effect that was rescued on addition of GSH (**Figure 3C**). Incubation of VLX1570 with recombinant CIAPIN1 showed similar higher MW complex formation (**Supplementary Figure 10A**) and formation of a covalent adduct was confirmed by electrospray mass spectrometry (MS) analysis (**Supplementary Figure 10B**). Further analysis by size exclusion chromatography demonstrated that these VLX1570 adducts result in the accumulation of protein aggregates (**Figure 4A**). LC-MS/MS analysis of the CIAPIN1-VLX1570 adduct following tryptic digest revealed that 7 out of a possible 10 cysteine residues were covalently modified by VLX1570, indicating that though VLX1570 modifies CIAPIN1 monomerically, it does so non-specifically (**Supplementary Figure 10C**). Closer inspection of an unmodified peptide containing Cys249 showed the presence of an intra-chain disulfide bond, which was disrupted in the equivalent VLX1570 modified peptide (**Supplementary Figure 11, Supplementary Table 2**). This disrupted disulfide bond represents one potential mechanism by which VLX1570 adducts result in CIAPIN1 instability and ultimately aggregation. Finally, we examined the fate of CIAPIN1 in intact cells following VLX1570 treatment. VLX1570 was titrated onto KMS11 cells and incubated for 1 or 6 hours before lysis and immunoblot analysis (**Figure 4B**). Aggregation was observed with 100 nM of VLX1570 after 1 hour, with

extended higher MW complexes and depletion of stable CIAPIN1 observed after 6 hours. This effect was conserved for b-AP15 (**Supplementary Figure 12**).

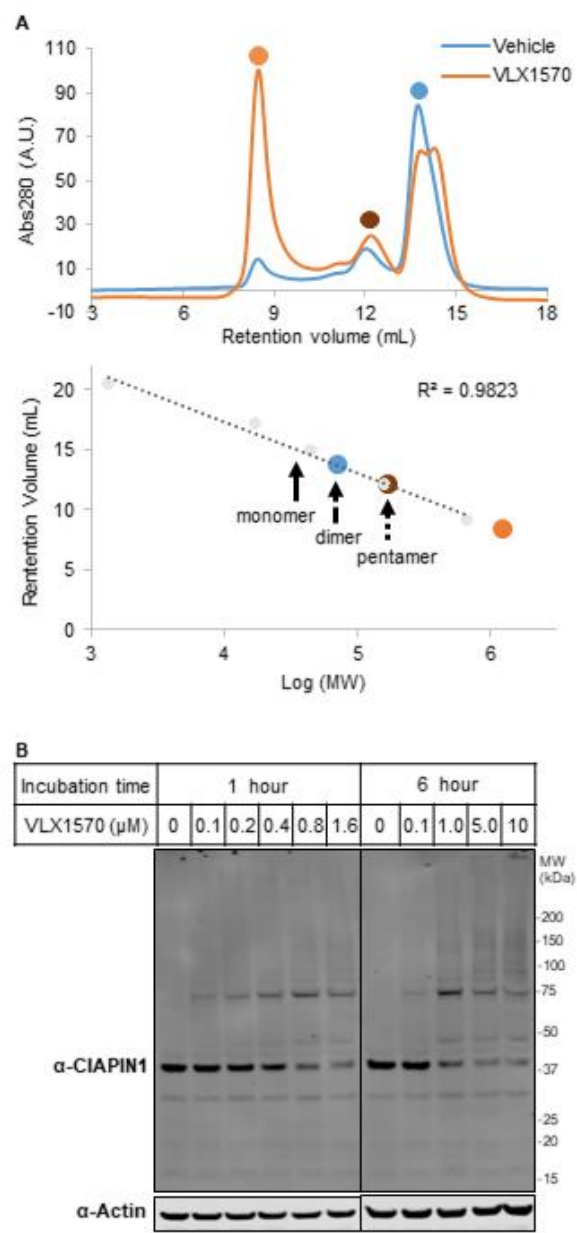


Figure 4. VLX1570 aggregates CIAPIN1. (A) Size exclusion chromatography of recombinant CIAPIN1 in the presence of VLX1570 or DMSO control indicates formation of an aggregation product. (B) Immunoblot analysis of high MW complex formation of CIAPIN1 following incubation with indicated concentrations of VLX1570 or DMSO

In summary, our data indicate that b-AP15 and VLX1570 react with multiple cellular proteins in a non-specific manner. Through a combination of immunoblot analysis and ABPP we have identified several additional DUB targets, and multiple proteins

unrelated to the ubiquitination machinery. Toxicity observed for drug candidates has been reported to be caused by off-target effects.³⁴ In the case of b-AP15 and VLX1570, we show that it is linked to the formation of high MW complexes following compound treatment, an effect that is abated by co-incubation with GSH. Other molecules like curcumin¹⁸ and its derivative AC17¹⁶, the diterpene NSC-302979¹⁸, synthetic compounds DBA¹⁸ and PYR-41¹⁴, the prostaglandin Δ 12-PGJ₂¹⁸, and the chalcone derivatives AM146¹⁷, RA-9¹⁷ and RA-14¹⁷, all contain α,β -unsaturated ketones and have been already described to inhibit isopeptidases. The affinity probe **1** has enabled the comprehensive profiling of the covalent targets of VLX1570 in intact cells, leading to the identification of CIAPIN1 as a target. Further analysis of CIAPIN1 has identified protein depletion through aggregation as a mode of action of VLX1570, supporting our observations with b-AP15.

Collectively, the data demonstrate the power of target profiling to elucidate mechanism of action and potential toxicity early in compound development. This strikes a cautionary note for the application of structurally similar compounds as tool compounds, and the clinical investigation of compounds possessing this chemotype.

Methods

Chemical synthesis and experimental procedures are included in the Supporting Information.

Data availability

The mass spectrometry proteomics data have been deposited to the ProteomeXchange Consortium via the PRIDE³⁵ partner repository with the dataset identifier PXD015412. Reviewers may access the data using the following credentials: Username: reviewer39460@ebi.ac.uk ; Password: 7Prr05Lq

Author information

*Corresponding authors: jennifer.ward@ndm.ox.ac.uk and adan.pintofernandez@ndm.ox.ac.uk contributed equally to the work. The authors declare no competing financial interests.

Acknowledgments

CIAPIN1 encoding pQTEV-LOC57019 was a gift from Konrad Buessow (Addgene plasmid # 34811; <http://n2t.net/addgene:34811>; RRID:Addgene_34811). JAW and KVMH are grateful for support by Myeloma UK (MUK). The SGC is a registered charity (number 1097737) that receives funds from AbbVie, Bayer Pharma AG, Boehringer Ingelheim, Canada Foundation for Innovation, Eshelman Institute for Innovation, Genome Canada, Innovative Medicines Initiative (EU/EFPIA) [ULTRA-DD grant no. 115766], Janssen, Merck KGaA Darmstadt Germany, MSD, Novartis Pharma AG, Ontario Ministry of Economic Development and Innovation, Pfizer, São Paulo Research Foundation-FAPESP, Takeda, and Wellcome [106169/ZZ14/Z]. APF, OF and OR's contributions to this study were supported by a grant from Innoviris (Région Bruxelles Capitale, Belgium).

References

1. Bergink, S.; Jentsch, S., Principles of ubiquitin and SUMO modifications in DNA repair. *Nature* **2009**, *458* (7237), 461-7.
2. Wertz, I. E.; Wang, X., From Discovery to Bedside: Targeting the Ubiquitin System. *Cell Chemical Biology* **2018**.
3. Jacq, X.; Kemp, M.; Martin, N. M.; Jackson, S. P., Deubiquitylating enzymes and DNA damage response pathways. *Cell Biochem Biophys* **2013**, *67* (1), 25-43.
4. Kategaya, L.; Di Lello, P.; Rougé, L.; Pastor, R.; Clark, K. R.; Drummond, J.; Kleinheinz, T.; Lin, E.; Upton, J.-P.; Prakash, S.; Heideker, J.; McClelland, M.; Ritorto, M. S.; Alessi, D. R.; Trost, M.; Bainbridge, T. W.; Kwok, M. C. M.; Ma, T. P.; Stiffler, Z.; Brasher, B.; Tang, Y.; Jaishankar, P.; Hearn, B. R.; Renslo, A. R.; Arkin, M. R.; Cohen, F.; Yu, K.; Peale, F.; Gnad, F.; Chang, M. T.; Klijn, C.; Blackwood, E.; Martin, S. E.; Forrest, W. F.; Ernst, J. A.; Ndubaku, C.; Wang, X.; Beresini, M. H.; Tsui, V.; Schwerdtfeger, C.; Blake, R. A.; Murray, J.; Maurer, T.; Wertz, I. E., USP7 small-molecule inhibitors interfere with ubiquitin binding. *Nature* **2017**, *550*, 534.
5. Turnbull, A. P.; Ioannidis, S.; Krajewski, W. W.; Pinto-Fernandez, A.; Heride, C.; Martin, A. C. L.; Tonkin, L. M.; Townsend, E. C.; Buker, S. M.; Lancia, D. R.; Caravella, J. A.; Toms, A. V.; Charlton, T. M.; Lahdenranta, J.; Wilker, E.; Follows, B. C.; Evans, N. J.; Stead, L.; Alli, C.; Zarayskiy, V. V.; Talbot, A. C.; Buckmelter, A. J.; Wang, M.; McKinnon, C. L.; Saab, F.; McGouran, J. F.; Century, H.; Gersch, M.; Pittman, M. S.; Marshall, C. G.; Raynham, T. M.; Simcox, M.; Stewart, L. M. D.; McLoughlin, S. B.; Escobedo, J. A.; Bair, K. W.; Dinsmore, C. J.; Hammonds, T. R.; Kim, S.; Urbe, S.; Clague, M. J.; Kessler, B. M.; Komander, D., Molecular basis of USP7 inhibition by selective small-molecule inhibitors. *Nature* **2017**, *550* (7677), 481-486.
6. van Esbroeck, A. C. M.; Janssen, A. P. A.; Cognetta, A. B., 3rd; Ogasawara, D.; Shpak, G.; van der Kroeg, M.; Kantae, V.; Baggelaar, M. P.; de Vrij, F. M. S.; Deng, H.; Allara, M.; Fezza, F.; Lin, Z.; van der Wel, T.; Soethoudt, M.; Mock, E. D.; den Dulk, H.; Baak, I. L.; Florea, B. I.; Hendriks, G.; De Petrocellis, L.; Overkleeft, H. S.; Hankemeier, T.; De Zeeuw, C. I.; Di Marzo, V.; Maccarrone, M.; Cravatt, B. F.; Kushner, S. A.; van der Stelt, M., Activity-based protein profiling reveals off-target proteins of the FAAH inhibitor BIA 10-2474. *Science* **2017**, *356* (6342), 1084-1087.
7. Altun, M.; Kramer, H. B.; Willems, L. I.; McDermott, J. L.; Leach, C. A.; Goldenberg, S. J.; Kumar, K. G.; Konietzny, R.; Fischer, R.; Kogan, E.; Mackeen, M. M.; McGouran, J.; Khoronenkova, S. V.; Parsons, J. L.; Dianov, G. L.; Nicholson, B.; Kessler, B. M., Activity-based chemical proteomics

accelerates inhibitor development for deubiquitylating enzymes. *Chemistry & biology* **2011**, *18* (11), 1401-12.

8. Ward, J. A.; McLellan, L.; Stockley, M.; Gibson, K. R.; Whitlock, G. A.; Knights, C.; Harrigan, J. A.; Jacq, X.; Tate, E. W., Quantitative Chemical Proteomic Profiling of Ubiquitin Specific Proteases in Intact Cancer Cells. *ACS Chem Biol* **2016**, *11* (12), 3268-3272.

9. Hewings, D. S.; Flygare, J. A.; Bogyo, M.; Wertz, I. E., Activity-based probes for the ubiquitin conjugation–deconjugation machinery: new chemistries, new tools, and new insights. *The FEBS Journal* **2017**, *284* (10), 1555-1576.

10. Lamberto, I.; Liu, X.; Seo, H. S.; Schauer, N. J.; Iacob, R. E.; Hu, W.; Das, D.; Mikhailova, T.; Weisberg, E. L.; Engen, J. R.; Anderson, K. C.; Chauhan, D.; Dhe-Paganon, S.; Buhrlage, S. J., Structure-Guided Development of a Potent and Selective Non-covalent Active-Site Inhibitor of USP7. *Cell chemical biology* **2017**, *24* (12), 1490-1500 e11.

11. D'Arcy, P.; Brnjic, S.; Olofsson, M. H.; Fryknas, M.; Lindsten, K.; De Cesare, M.; Perego, P.; Sadeghi, B.; Hassan, M.; Larsson, R.; Linder, S., Inhibition of proteasome deubiquitinating activity as a new cancer therapy. *Nat Med* **2011**, *17* (12), 1636-40.

12. Tian, Z.; D'Arcy, P.; Wang, X.; Ray, A.; Tai, Y. T.; Hu, Y.; Carrasco, R. D.; Richardson, P.; Linder, S.; Chauhan, D.; Anderson, K. C., A novel small molecule inhibitor of deubiquitylating enzyme USP14 and UCHL5 induces apoptosis in multiple myeloma and overcomes bortezomib resistance. *Blood* **2014**, *123* (5), 706-16.

13. de Jong, A.; Merckx, R.; Berlin, I.; Rodenko, B.; Wijdeven, R. H.; El Atmioui, D.; Yalcin, Z.; Robson, C. N.; Neefjes, J. J.; Ovaa, H., Ubiquitin-based probes prepared by total synthesis to profile the activity of deubiquitinating enzymes. *Chembiochem : a European journal of chemical biology* **2012**, *13* (15), 2251-8.

14. Kapuria, V.; Peterson, L. F.; Showalter, H. D.; Kirchhoff, P. D.; Talpaz, M.; Donato, N. J., Protein cross-linking as a novel mechanism of action of a ubiquitin-activating enzyme inhibitor with anti-tumor activity. *Biochemical pharmacology* **2011**, *82* (4), 341-9.

15. D'Arcy, P.; Linder, S., Proteasome deubiquitinases as novel targets for cancer therapy. *Int.J.Biochem.Cell Biol.* **2012**, *44* (11), 1729-1738.

16. Zhou, B.; Zuo, Y.; Li, B.; Wang, H.; Liu, H.; Wang, X.; Qiu, X.; Hu, Y.; Wen, S.; Du, J.; Bu, X., Deubiquitinase inhibition of 19S regulatory particles by 4-arylidene curcumin analog AC17 causes NF-kappaB inhibition and p53 reactivation in human lung cancer cells. *Molecular cancer therapeutics* **2013**, *12* (8), 1381-92.

17. Issaenko, O. A.; Amerik, A. Y., Chalcone-based small-molecule inhibitors attenuate malignant phenotype via targeting deubiquitinating enzymes. *Cell Cycle* **2012**, *11* (9), 1804-17.

18. Mullally, J. E.; Fitzpatrick, F. A., Pharmacophore model for novel inhibitors of ubiquitin isopeptidases that induce p53-independent cell death. *Molecular pharmacology* **2002**, *62* (2), 351-8.

19. Pinto, A.; Mace, Y.; Drouet, F.; Bony, E.; Boidot, R.; Draoui, N.; Lobysheva, I.; Corbet, C.; Polet, F.; Martherus, R.; Deraedt, Q.; Rodríguez, J.; Lamy, C.; Schicke, O.; Delvaux, D.; Louis, C.; Kiss, R.; Kriegsheim, A. V.; Dessy, C.; Elias, B.; Quetin-Leclercq, J.; Riant, O.; Feron, O., A new ER-specific photosensitizer unravels 1O₂-driven protein oxidation and inhibition of deubiquitinases as a generic mechanism for cancer PDT. *Oncogene* **2015**, *35*, 3976.

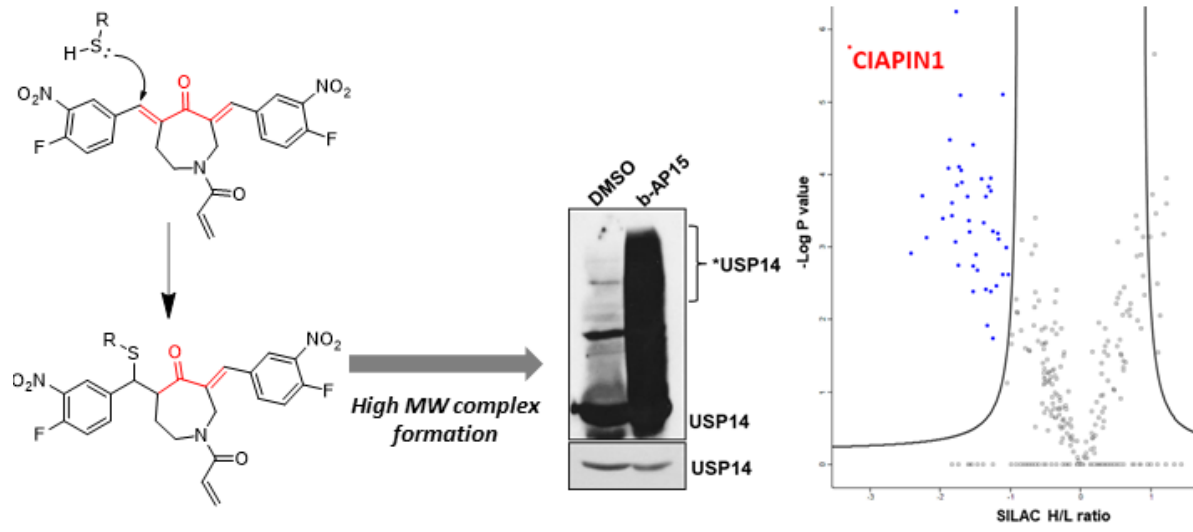
20. Wang, X.; D'Arcy, P.; Caulfield, T. R.; Paulus, A.; Chitta, K.; Mohanty, C.; Gullbo, J.; Chanan-Khan, A.; Linder, S., Synthesis and evaluation of derivatives of the proteasome deubiquitinase inhibitor b-AP15. *Chem Biol Drug Des* **2015**, *86* (5), 1036-48.

21. Wang, X.; Mazurkiewicz, M.; Hillert, E. K.; Olofsson, M. H.; Pierrou, S.; Hillertz, P.; Gullbo, J.; Selvaraju, K.; Paulus, A.; Akhtar, S.; Bossler, F.; Khan, A. C.; Linder, S.; D'Arcy, P., The proteasome deubiquitinase inhibitor VLX1570 shows selectivity for ubiquitin-specific protease-14 and induces apoptosis of multiple myeloma cells. *Sci Rep* **2016**, *6*, 26979.

22. Borodovsky, A.; Ovaa, H.; Kolli, N.; Gan-Erdene, T.; Wilkinson, K. D.; Ploegh, H. L.; Kessler, B. M., Chemistry-based functional proteomics reveals novel members of the deubiquitinating enzyme family. *Chem Biol* **2002**, *9* (10), 1149-59.

23. Weerapana, E.; Simon, G. M.; Cravatt, B. F., Disparate proteome reactivity profiles of carbon electrophiles. *Nat Chem Biol* **2008**, *4* (7), 405-7.
24. Heal, W. P.; Jovanovic, B.; Bessin, S.; Wright, M. H.; Magee, A. I.; Tate, E. W., Bioorthogonal chemical tagging of protein cholesterylization in living cells. *Chem Commun (Camb)* **2011**, *47* (14), 4081-3.
25. Geiger, T.; Wisniewski, J. R.; Cox, J.; Zanivan, S.; Kruger, M.; Ishihama, Y.; Mann, M., Use of stable isotope labeling by amino acids in cell culture as a spike-in standard in quantitative proteomics. *Nat Protoc* **2011**, *6* (2), 147-57.
26. Sadaghiani, A. M.; Verhelst, S. H.; Bogoy, M., Tagging and detection strategies for activity-based proteomics. *Curr Opin Chem Biol* **2007**, *11* (1), 20-8.
27. Banci, L.; Bertini, I.; Calderone, V.; Ciofi-Baffoni, S.; Giachetti, A.; Jaiswal, D.; Mikolajczyk, M.; Piccioli, M.; Winkelmann, J., Molecular view of an electron transfer process essential for iron-sulfur protein biogenesis. *Proceedings of the National Academy of Sciences* **2013**, *110* (18), 7136.
28. Song, G.; Cheng, C.; Li, Y.; Shaw, N.; Xiao, Z. C.; Liu, Z. J., Crystal structure of the N-terminal methyltransferase-like domain of anamorsin. *Proteins* **2014**, *82* (6), 1066-71.
29. Shibayama, H.; Takai, E.; Matsumura, I.; Kouno, M.; Morii, E.; Kitamura, Y.; Takeda, J.; Kanakura, Y., Identification of a Cytokine-induced Antiapoptotic Molecule Anamorsin Essential for Definitive Hematopoiesis. *The Journal of Experimental Medicine* **2004**, *199* (4), 581.
30. Wang, J.; Li, Q.; Wang, C.; Xiong, Q.; Lin, Y.; Sun, Q.; Jin, H.; Yang, F.; Ren, X.; Pang, T., Knock-down of CIAPIN1 sensitizes K562 chronic myeloid leukemia cells to Imatinib by regulation of cell cycle and apoptosis-associated members via NF-kappaB and ERK5 signaling pathway. *Biochem Pharmacol* **2016**, *99*, 132-45.
31. Li, X.; Pan, Y.; Fan, R.; Jin, H.; Han, S.; Liu, J.; Wu, K.; Fan, D., Adenovirus-delivered CIAPIN1 small interfering RNA inhibits HCC growth in vitro and in vivo. *Carcinogenesis* **2008**, *29* (8), 1587-93.
32. Zhao, Y.; Wei Eric, W.; Qian, Z., CIAPIN1 siRNA Inhibits Proliferation, Migration and Promotes Apoptosis of VSMCs by Regulating Bcl-2 and Bax. *Current Neurovascular Research* **2013**, *10* (1), 4-10.
33. Zhang, Y.; Fang, J.; Ma, H., Inhibition of miR-182-5p protects cardiomyocytes from hypoxia-induced apoptosis by targeting CIAPIN1. *Biochem Cell Biol* **2018**, *96* (5), 646-654.
34. Lin, A.; Giuliano, C. J.; Palladino, A.; John, K. M.; Abramowicz, C.; Yuan, M. L.; Sausville, E. L.; Lukow, D. A.; Liu, L.; Chait, A. R.; Galluzzo, Z. C.; Tucker, C.; Sheltzer, J. M., Off-target toxicity is a common mechanism of action of cancer drugs undergoing clinical trials. *Sci Transl Med* **2019**, *11* (509).
35. Perez-Riverol, Y.; Csordas, A.; Bai, J.; Bernal-Llinares, M.; Hewapathirana, S.; Kundu, D. J.; Inuganti, A.; Griss, J.; Mayer, G.; Eisenacher, M.; Perez, E.; Uszkoreit, J.; Pfeuffer, J.; Sachsenberg, T.; Yilmaz, S.; Tiwary, S.; Cox, J.; Audain, E.; Walzer, M.; Jarnuczak, A. F.; Ternent, T.; Brazma, A.; Vizcaino, J. A., The PRIDE database and related tools and resources in 2019: improving support for quantification data. *Nucleic Acids Res* **2019**, *47* (D1), D442-D450.

TOC



VLX_Manuscript_Submission.pdf (885.02 KiB)

[view on ChemRxiv](#) • [download file](#)

Re-evaluating the mechanism of action of α,β -unsaturated carbonyl DUB inhibitors b-AP15 and VLX1570: a paradigmatic example of unspecific protein crosslinking with Michael acceptor motif-containing drugs.

Jennifer A. Ward,^{1,2,5*} Adan Pinto-Fernandez,^{2,4*} Loïc Cornelissen,³ Sarah Bonham,² Laura Díaz-Sáez,^{1,2} Olivier Riant,⁴ Kilian V. M. Huber,^{1,2} Benedikt M. Kessler,² Olivier Feron,³ and Edward W. Tate⁵

¹Structural Genomics Consortium, Nuffield Department of Medicine, University of Oxford, Oxford, UK.

²Target Discovery Institute, Nuffield Department of Medicine, University of Oxford, Oxford, UK.

³Institute of Condensed Matter and Nanosciences Molecules, Solids and Reactivity (IMCN/MOST), UCLouvain, Brussels, Belgium.

⁴Pole of Pharmacology and Therapeutics (FATH), Institut de Recherche Expérimentale et Clinique (IREC), UCLouvain, Brussels, Belgium.

⁵Department of Chemistry, Imperial College London, Molecular Sciences Research Hub, White City Campus, London, UK.

*Corresponding authors: jennifer.ward@ndm.ox.ac.uk and adan.pintofernandez@ndm.ox.ac.uk

Abstract

Deubiquitinating enzymes are a growing target class across multiple disease states, with several inhibitors now reported. b-AP15 and VLX1570 are two structurally related USP14/UCH-37 inhibitors with a shared α,β -unsaturated carbonyl substructure motif. Initially taken forward into a phase I/II clinical trial for refractory multiple myeloma, VLX1570 has since been put on full clinical hold due to dose limiting toxicity. Through a proteomic approach, here we demonstrate that these compounds target a diverse range of proteins, resulting in the formation of higher molecular weight complexes. Activity-based proteome profiling identified CIAPIN1 as a sub-micromolar covalent target of VLX1570, and further analysis demonstrated that high molecular weight complex formation leads to aggregation of CIAPIN1 in intact cells. Our results suggest that in addition to DUB inhibition, these compounds induce non-specific protein aggregation through cross-linking, providing a molecular explanation for general cellular toxicity.

Main

Ubiquitination, the covalent addition of the 76 amino acid protein ubiquitin (Ub) to protein substrates, is a widespread protein post-translational modification (PTM) in eukaryotic cells.¹ Due to its role in proteasomal degradation and a plethora of signalling pathways, ubiquitination is an emerging field of clinical interest in multiple

disease states, including cancer.²⁻⁴ Several compounds have been reported in recent years targeting deubiquitinating enzymes (DUBs)^{4,5} which regulate the removal of Ub marks. However, the characterisation of such inhibitors and clinical compounds from a target perspective is variable; though a DUB target is reported, compound selectivity and specificity across the proteome remained in most cases incompletely resolved. Comprehensive understanding of a compound's targets facilitates interpretation of phenotypes in pre-clinical investigations, and can identify mechanisms of toxicity⁶ and resistance at an early stage of testing. Only recently, and with the help of advanced activity-based protein profiling (ABPP)⁷⁻⁹ assays that allow the profiling of DUBs in a cellular context, highly selective DUB inhibitors have been reported.^{4,5,10} Here, we describe the proteomic investigation of two structurally related DUB inhibitors b-AP15 and VLX1570. We demonstrate that these inhibitors target a diverse range of proteins, resulting in the formation of higher molecular weight (MW) complexes. Through a quantitative chemical proteomic approach, we identify CIAPIN1, also known as anamorsin, as a potent covalent target of VLX1570 which upon reaction with VLX1570 forms high molecular weight complexes leading to aggregation of CIAPIN1 in intact cells.

b-AP15 has been previously described as a specific reversible inhibitor of the proteasomal DUBs USP14 and UCH-37 (also referred to as UCH-L5) with anti-cancer activities.^{11,12} Examination of the chemical structure of b-AP15, however, shows the presence of Michael acceptor motifs (**Figure 1A**) that are capable of covalent interaction with nucleophilic residues. Although the results obtained by D'Arcy and colleagues demonstrate that b-AP15 is an inhibitor of USP14/UCH-37,¹¹ two unrelated cysteine protease enzymes from different DUB families, its structure suggests additional proteins may be targeted by this compound class. Indeed, b-AP15 possesses higher potency in intact cells than in biophysical assays against USP14 and UCH-37.¹¹ In support of compound promiscuity, another study describing the chemical synthesis of active-site-directed DUB probes showed data compatible with a non-specific DUB inhibition profile upon increasing concentrations of b-AP15.¹³ In our hands, b-AP15 inhibits the cleavage of the DUB substrate Ub-AML (ubiquitin-aminoluciferin) by a number of purified recombinant DUBs (**Figure 1B**). Crude extracts of cells treated with increasing concentrations of b-AP15 also

showed that b-AP15 is able to decrease the global DUB activity of these treated cells (**Figure 1C**). Further, b-AP15 treatment in both cancer cell lines and endothelial cells resulted in comparable cytotoxicity as observed by a cell viability assay, indicating the non-specific toxicity of this chemotype (**Supplementary Figure 1**).

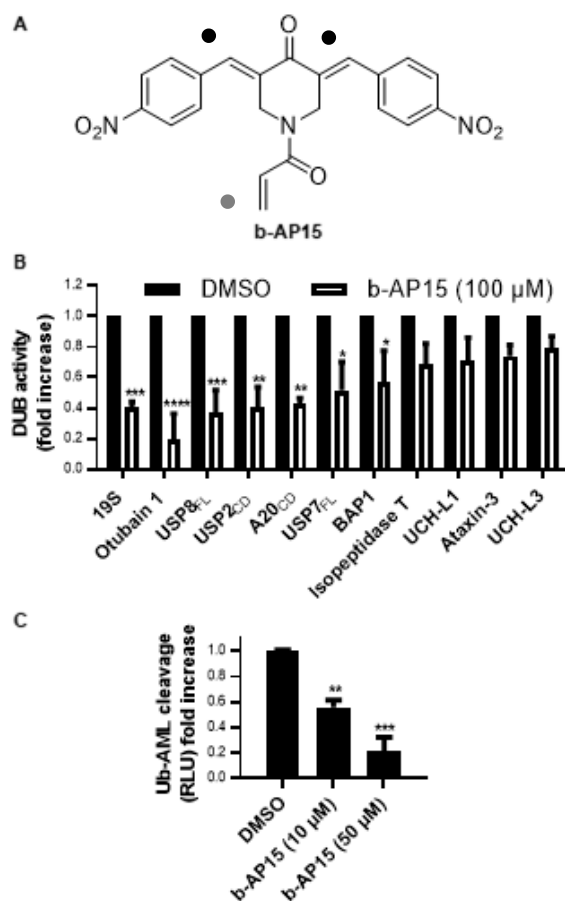


Figure 1. b-AP15 is a non-specific deubiquitinating enzyme (DUB) inhibitor. (A) Molecular structure of b-AP15 with Michael acceptors (black dot) and acrylamide (grey dot) motif indicated. (B) DUB activity measured by cleavage of the luminescent substrate Ub-AML in a panel of recombinant proteasomal (purified 19S proteasomes) and non-proteasomal DUBs treated with b-AP15 (100 μM) (n=3-4). (C) DUB assay as described above using HeLa cell extracts (5 μg) incubated with the indicated b-AP15 concentrations (n=3).

By immunoblot analysis, it was observed that b-AP15 induces the formation of high MW complexes with USP14 (**Figure 2A and 2B**) and UCH-37 (**Supplementary Figure 2**) in both crude cell extracts and intact cells. The formation of these complexes is reduced by co-incubation with thiol containing reducing reagents DTT or GSH, in support of these higher MW complexes forming via the Michael acceptors. The protective effect of these reagents was hypothesized to be due to the blocking of these reactive sites. To test this, b-AP15 was reacted *in vitro* with an

excess of GSH in PBS, representing conditions similar to those used in our *in vitro* and *in situ* assays. As predicted, b-AP15(GSH)₂ could be observed by LC-MS analysis after 1 hour of incubation. (**Supplementary Figure 3**). In support of this finding, PYR-41, an ubiquitin-activating enzyme (E1) inhibitor (also containing Michael acceptors), has been reported to induce DTT-sensitive protein cross-linking and inhibition of DUBs and other cellular enzymes by formation of high MW complexes¹⁴. In addition, high MW ubiquitylated proteins accumulated upon b-AP15 treatment, the levels of which were reduced by co-treatment with DTT and GSH (**Figure 2C**). The origin of these very high molecular weight ubiquitylated proteins that accumulate upon treatment with b-AP15 in comparison with those that accumulate on application of proteasome inhibitors has been largely discussed.^{11, 15} Interestingly, ubiquitylated protein complexes with very high MW are also reported by D'Arcy and other studies using α,β unsaturated carbonyl compounds.^{14, 16-18} The effects of b-AP15 on the global proteome were further evaluated by SDS-PAGE followed by Coomassie Blue staining, revealing the formation of notably increased levels of high MW protein complexes in comparison to DMSO control or co-treatment with DTT and GSH (**Figure 2D**). To better characterize the consequences of the global formation of high MW protein complexes on cell signalling, the status of mTOR was analysed in crude extracts treated with b-AP15 by immunoblotting. Strikingly, a shift from mTOR in its native form towards a band with slower migration mobility is observed with nanomolar concentration of bAP-15 (**Supplementary Figure 4A and 4B**). A similar observation was described by us in a previous study showing oxidation of proteins by a photosensitiser.¹⁹ A similar but less potent effect was observed on incubation with the natural product curcumin, which also possesses Michael acceptor groups (**Supplementary Figure 4C and 4D**).

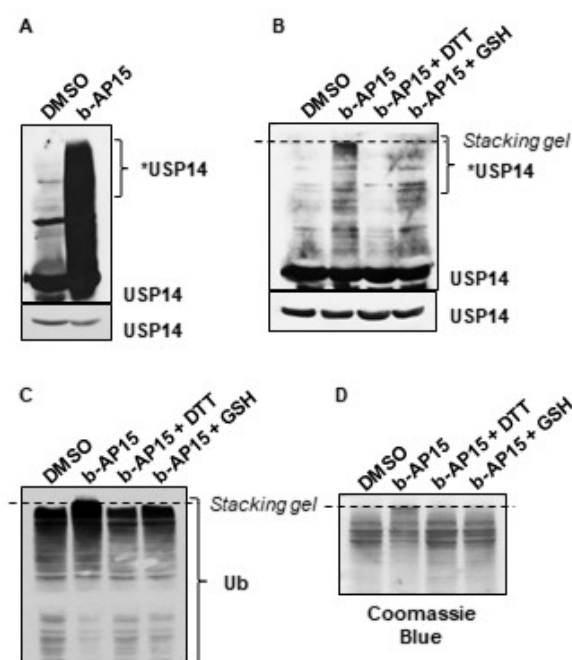


Figure 2. b-AP15 inhibits DUBs through the formation of cytotoxic high MW protein complexes, which are averted in the presence of thiol reducing agents. Immunoblot analysis of high MW complexes of USP14 in (A) HeLa crude cell extracts incubated with b-AP15 (10 μ M) and in (B) HeLa cells treated with either vehicle, 10 μ M b-AP15 or with 10 μ M b-AP15 in combination with reducing agents (10 mM dithiothreitol (DTT) or 10 mM glutathione (GSH)), both at 37°C for 2 hours. Shorter exposure times were used as a loading control (lower blots in the panel). (C) Immunoblot analysis of ubiquitin conjugates in HeLa cells treated with vehicle, 10 μ M b-AP15, or with 10 μ M b-AP15 in combination with reducing agents (10 mM dithiothreitol (DTT) or 10 mM glutathione (GSH)) for 2 hours. (D) Visualization of the b-AP15-induced high MW protein complexes in a SDS-PAGE gel, after Coomassie Blue staining, in HeLa cells treated as in (C).

VLX1570 is a structural analogue of b-AP-15 that shows higher potency and improved permeability.^{20, 21} VLX1570 was taken forward into a phase I/II clinical trial for refractory multiple myeloma in combination with dexamethasone (NCT02372240), but was then put on full clinical hold in July 2017 due to dose limiting toxicity. Based on our analysis of b-AP15, we postulated that this toxicity may be due to promiscuous covalent reaction with cellular nucleophiles and formation of high MW complexes. To test whether VLX1570 also forms high MW complexes, HeLa lysates were treated with varying concentrations of b-AP15 and VLX1570 and probed with the active-site-directed DUB probe HA-Ub-C2Br.²² Dose-dependent inhibition of probe labelling was observed for both compounds. Even on blotting for USP28, a DUB structurally unrelated to both USP14 and UCH-37, higher MW complex formation was observed (**Supplementary Figure 5**). Co-incubation of both VLX1570 and b-AP15 with GSH in the multiple myeloma cell line KMS11 led to increased cell

viability after 16 hours, suggesting that the GSH is scavenging these compounds and reducing their active concentration (**Supplementary Figure 6**).

GSH represents one of many nucleophiles accessible to VLX1570 within a biological context, and Michael acceptors are well known for their reactivity with cysteine residues.²³ To comprehensively profile the covalent targets of VLX1570, ABPP was conducted. Accordingly, an alkyne tagged analogue of VLX1570, Compound **1** (**Figure 3A**) was designed and synthesized. The acrylamide position was selected for conversion to the alkyne, as acrylamide-lacking analogues had previously been reported in structure-activity relationship studies not to influence cell viability.²⁰ Indeed, **1** retained equivalent cytotoxicity to VLX1570 in both KMS11 and U2OS cell lines, as observed with the CellTiter Glo assay (**Figure 3A, Supplementary Figure 7**).

Before commencing proteomic-profiling experiments, suitable competitive conditions were determined. U2OS cells were pre-incubated with increasing concentrations of VLX1570 or bAP-15 for 30 minutes before addition of the affinity probe **1** at a final concentration of 5 μ M. After 1 hour, the cells were lysed. Subsequent ligation to AzTB,²⁴ an azido-TAMRA-biotin capture reagent, via a copper catalyzed azide-alkyne cycloaddition (CuAAC) allowed visualization of probe-protein complexes by in-gel fluorescence. Both VLX1570 and b-AP15 pre-incubation caused a reduction in labelling intensity for specific bands, most markedly affecting a band at approximately 37 kDa (**Supplementary Figure 8A**). 5 and 20 μ M VLX1570 competitive conditions were taken forward for proteomic analysis. Spike-in SILAC methodology²⁵ was employed as previously described.^{8, 26} Briefly, cell lysates from competitive conditions were mixed in a 2:1 ratio with 'spike': lysate generated from **1**-treated U2OS cells grown in R10K8 media. Subsequent CuAAC ligation, enrichment on NeutrAvidin-Agarose resin, tryptic digest and LC-MS/MS analysis enabled proteome-wide in-cell target identification of **1**-labelled proteins. Multiple covalent targets were identified using this method, with significant competition observed at both 1- and 4-fold competitor excess. 44 proteins were significantly competed by 20 μ M VLX1570 (**Figure 3B, Supporting Dataset 1**), 24 of which were also significantly competed by 5 μ M of compound (**Supplementary Figure 8B**). On inspection of these protein sequences, all contained cysteine residues. Gene Ontology cellular component analysis suggested that VLX1570 was covalently interacting with proteins across multiple cellular locations, including the cytoplasm,

nucleus, and multiple organelles (**Supplementary Table 1**). It should be noted that although we have demonstrated accumulation of higher MW bands for UCH-37, USP14 and USP28 by immunoblot analysis, none of these DUBs were identified in the ABPP experiment. As the ABPP experiment only identifies covalent interactors, it is possible that the high MW complex formation observed for DUBs is occurring through a non-covalent mechanism. This is in agreement with literature data reporting that although DTT does affect cytotoxicity of VLX1570²⁰, compound binding and enzymatic inhibition are both reversible.²¹ Alternatively, it is possible that the high MW complexes formed with these proteins sterically hinder the CuAAC ligation reaction, thereby preventing covalently **1**-labelled proteins from being enriched and identified in this experiment.

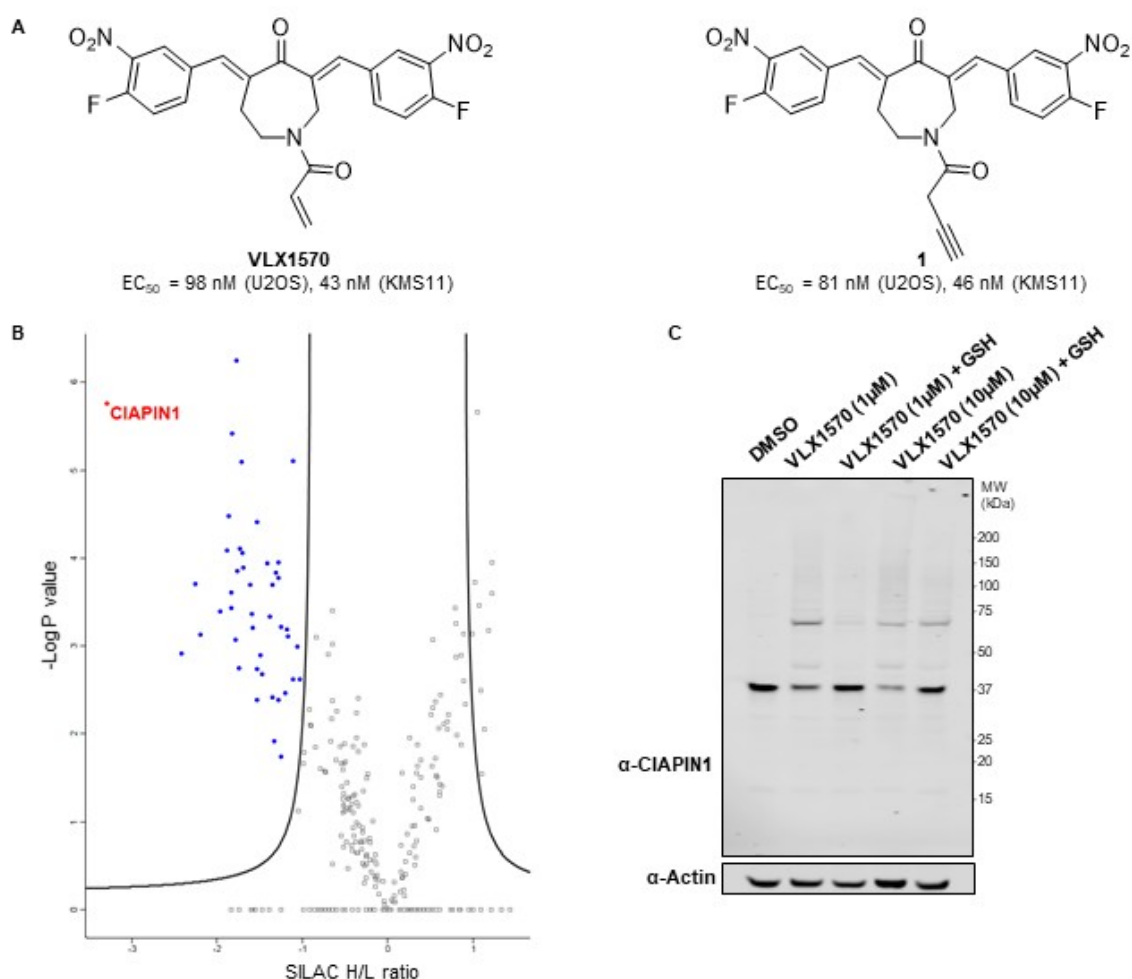


Figure 3. Chemical proteomics reveals multiple covalent targets of VLX1570. (A) Structure of VLX1570 and probe derivative compound **1**. EC₅₀ values measured by CellTiter Glo in U2OS and KMS11 cells are reported. (B) Volcano plot of **1**-enriched proteome from U2OS cells, with targets significantly (FDR=0.05, S0 = 0.2) competed by 20 μM VLX1570 indicated (blue). The most significant

hit, CIAPIN1, is indicated. **(C)** Immunoblot analysis of VLX1570 treated KMS11 cells demonstrates a protective effect against high MW complex formation for CIAPIN1 on addition of GSH (10 mM, 2 hr).

The most significantly competed covalent target of VLX1570 identified was CIAPIN1. CIAPIN1, a 33 kDa protein, is a part of the electron transport chain that enables Fe-S cluster assembly.²⁷ It possesses an N-methyltransferase domain at its N-terminus, though this has been reported to be catalytically inactive.²⁸ Further, CIAPIN1 exerts anti-apoptotic effects in cells though it is unrelated to apoptosis regulatory molecules of the BCL2 or CASP families.²⁹ In our hands, siRNA knockdown of CIAPIN1 lead to a reduction in cell viability of KMS11 cells (**Supplementary Figure 9**). Knockdown of CIAPIN1 has been reported to induce apoptosis in several cancer^{30, 31} and also non-cancer cell lines.^{32, 33} In agreement with functional inhibition of CIAPIN1, both b-AP15 and VLX1570 are reported to exert cytotoxicity via an apoptotic mechanism that is insensitive to BCL2 overexpression.^{11, 21}

As observed for DUB targets of this chemotype, higher MW complex formation was observed on immunoblotting for CIAPIN1 in VLX1570 treated cells, an effect that was rescued on addition of GSH (**Figure 3C**). Incubation of VLX1570 with recombinant CIAPIN1 showed similar higher MW complex formation (**Supplementary Figure 10A**) and formation of a covalent adduct was confirmed by electrospray mass spectrometry (MS) analysis (**Supplementary Figure 10B**). Further analysis by size exclusion chromatography demonstrated that these VLX1570 adducts result in the accumulation of protein aggregates (**Figure 4A**). LC-MS/MS analysis of the CIAPIN1-VLX1570 adduct following tryptic digest revealed that 7 out of a possible 10 cysteine residues were covalently modified by VLX1570, indicating that though VLX1570 modifies CIAPIN1 monomerically, it does so non-specifically (**Supplementary Figure 10C**). Closer inspection of an unmodified peptide containing Cys249 showed the presence of an intra-chain disulfide bond, which was disrupted in the equivalent VLX1570 modified peptide (**Supplementary Figure 11, Supplementary Table 2**). This disrupted disulfide bond represents one potential mechanism by which VLX1570 adducts result in CIAPIN1 instability and ultimately aggregation. Finally, we examined the fate of CIAPIN1 in intact cells following VLX1570 treatment. VLX1570 was titrated onto KMS11 cells and incubated for 1 or 6 hours before lysis and immunoblot analysis (**Figure 4B**). Aggregation was observed with 100 nM of VLX1570 after 1 hour, with

extended higher MW complexes and depletion of stable CIAPIN1 observed after 6 hours. This effect was conserved for b-AP15 (**Supplementary Figure 12**).

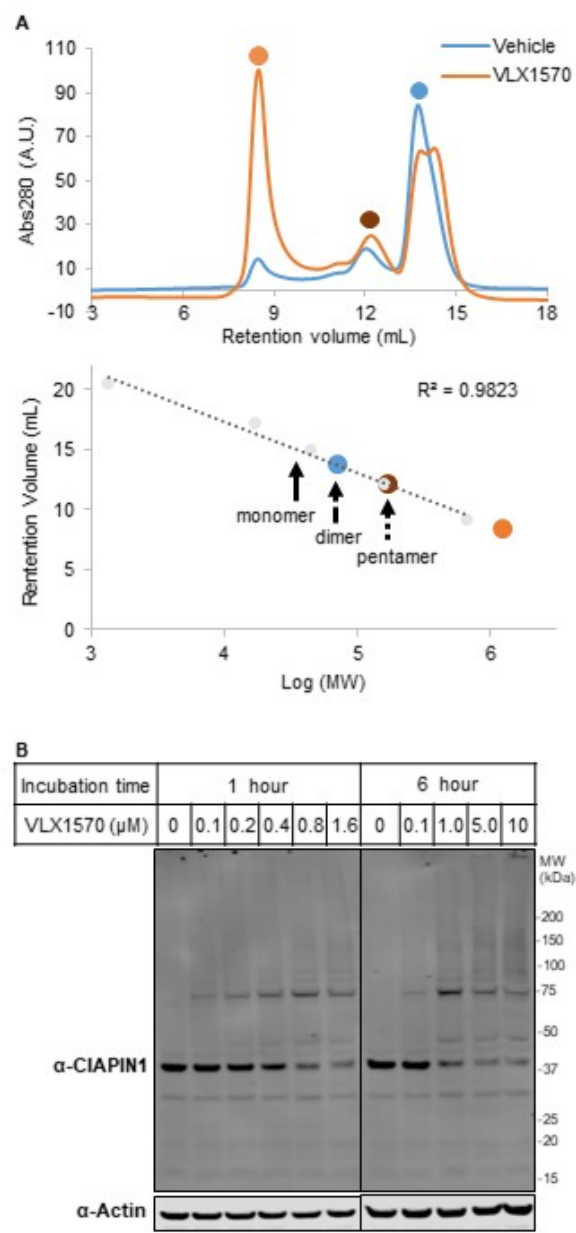


Figure 4. VLX1570 aggregates CIAPIN1. (A) Size exclusion chromatography of recombinant CIAPIN1 in the presence of VLX1570 or DMSO control indicates formation of an aggregation product. (B) Immunoblot analysis of high MW complex formation of CIAPIN1 following incubation with indicated concentrations of VLX1570 or DMSO

In summary, our data indicate that b-AP15 and VLX1570 react with multiple cellular proteins in a non-specific manner. Through a combination of immunoblot analysis and ABPP we have identified several additional DUB targets, and multiple proteins

unrelated to the ubiquitination machinery. Toxicity observed for drug candidates has been reported to be caused by off-target effects.³⁴ In the case of b-AP15 and VLX1570, we show that it is linked to the formation of high MW complexes following compound treatment, an effect that is abated by co-incubation with GSH. Other molecules like curcumin¹⁸ and its derivative AC17¹⁶, the diterpene NSC-302979¹⁸, synthetic compounds DBA¹⁸ and PYR-41¹⁴, the prostaglandin Δ 12-PGJ₂¹⁸, and the chalcone derivatives AM146¹⁷, RA-9¹⁷ and RA-14¹⁷, all contain α,β -unsaturated ketones and have been already described to inhibit isopeptidases. The affinity probe **1** has enabled the comprehensive profiling of the covalent targets of VLX1570 in intact cells, leading to the identification of CIAPIN1 as a target. Further analysis of CIAPIN1 has identified protein depletion through aggregation as a mode of action of VLX1570, supporting our observations with b-AP15.

Collectively, the data demonstrate the power of target profiling to elucidate mechanism of action and potential toxicity early in compound development. This strikes a cautionary note for the application of structurally similar compounds as tool compounds, and the clinical investigation of compounds possessing this chemotype.

Methods

Chemical synthesis and experimental procedures are included in the Supporting Information.

Data availability

The mass spectrometry proteomics data have been deposited to the ProteomeXchange Consortium via the PRIDE³⁵ partner repository with the dataset identifier PXD015412. Reviewers may access the data using the following credentials: Username: reviewer39460@ebi.ac.uk ; Password: 7PPro5Lq

Author information

*Corresponding authors: jennifer.ward@ndm.ox.ac.uk and adan.pintofernandez@ndm.ox.ac.uk contributed equally to the work. The authors declare no competing financial interests.

Acknowledgments

CIAPIN1 encoding pQTEV-LOC57019 was a gift from Konrad Buessow (Addgene plasmid # 34811; <http://n2t.net/addgene:34811>; RRID:Addgene_34811). JAW and KVMH are grateful for support by Myeloma UK (MUK). The SGC is a registered charity (number 1097737) that receives funds from AbbVie, Bayer Pharma AG, Boehringer Ingelheim, Canada Foundation for Innovation, Eshelman Institute for Innovation, Genome Canada, Innovative Medicines Initiative (EU/EFPIA) [ULTRA-DD grant no. 115766], Janssen, Merck KGaA Darmstadt Germany, MSD, Novartis Pharma AG, Ontario Ministry of Economic Development and Innovation, Pfizer, São Paulo Research Foundation-FAPESP, Takeda, and Wellcome [106169/ZZ14/Z]. APF, OF and OR's contributions to this study were supported by a grant from Innoviris (Région Bruxelles Capitale, Belgium).

References

1. Bergink, S.; Jentsch, S., Principles of ubiquitin and SUMO modifications in DNA repair. *Nature* **2009**, *458* (7237), 461-7.
2. Wertz, I. E.; Wang, X., From Discovery to Bedside: Targeting the Ubiquitin System. *Cell Chemical Biology* **2018**.
3. Jacq, X.; Kemp, M.; Martin, N. M.; Jackson, S. P., Deubiquitylating enzymes and DNA damage response pathways. *Cell Biochem Biophys* **2013**, *67* (1), 25-43.
4. Kategaya, L.; Di Lello, P.; Rougé, L.; Pastor, R.; Clark, K. R.; Drummond, J.; Kleinheinz, T.; Lin, E.; Upton, J.-P.; Prakash, S.; Heideker, J.; McClelland, M.; Ritorto, M. S.; Alessi, D. R.; Trost, M.; Bainbridge, T. W.; Kwok, M. C. M.; Ma, T. P.; Stiffler, Z.; Brasher, B.; Tang, Y.; Jaishankar, P.; Hearn, B. R.; Renslo, A. R.; Arkin, M. R.; Cohen, F.; Yu, K.; Peale, F.; Gnad, F.; Chang, M. T.; Klijn, C.; Blackwood, E.; Martin, S. E.; Forrest, W. F.; Ernst, J. A.; Ndubaku, C.; Wang, X.; Beresini, M. H.; Tsui, V.; Schwerdtfeger, C.; Blake, R. A.; Murray, J.; Maurer, T.; Wertz, I. E., USP7 small-molecule inhibitors interfere with ubiquitin binding. *Nature* **2017**, *550*, 534.
5. Turnbull, A. P.; Ioannidis, S.; Krajewski, W. W.; Pinto-Fernandez, A.; Heride, C.; Martin, A. C. L.; Tonkin, L. M.; Townsend, E. C.; Buker, S. M.; Lancia, D. R.; Caravella, J. A.; Toms, A. V.; Charlton, T. M.; Lahdenranta, J.; Wilker, E.; Follows, B. C.; Evans, N. J.; Stead, L.; Alli, C.; Zarayskiy, V. V.; Talbot, A. C.; Buckmelter, A. J.; Wang, M.; McKinnon, C. L.; Saab, F.; McGouran, J. F.; Century, H.; Gersch, M.; Pittman, M. S.; Marshall, C. G.; Raynham, T. M.; Simcox, M.; Stewart, L. M. D.; McLoughlin, S. B.; Escobedo, J. A.; Bair, K. W.; Dinsmore, C. J.; Hammonds, T. R.; Kim, S.; Urbe, S.; Clague, M. J.; Kessler, B. M.; Komander, D., Molecular basis of USP7 inhibition by selective small-molecule inhibitors. *Nature* **2017**, *550* (7677), 481-486.
6. van Esbroeck, A. C. M.; Janssen, A. P. A.; Cognetta, A. B., 3rd; Ogasawara, D.; Shpak, G.; van der Kroeg, M.; Kantae, V.; Baggelaar, M. P.; de Vrij, F. M. S.; Deng, H.; Allara, M.; Fezza, F.; Lin, Z.; van der Wel, T.; Soethoudt, M.; Mock, E. D.; den Dulk, H.; Baak, I. L.; Florea, B. I.; Hendriks, G.; De Petrocellis, L.; Overkleeft, H. S.; Hankemeier, T.; De Zeeuw, C. I.; Di Marzo, V.; Maccarrone, M.; Cravatt, B. F.; Kushner, S. A.; van der Stelt, M., Activity-based protein profiling reveals off-target proteins of the FAAH inhibitor BIA 10-2474. *Science* **2017**, *356* (6342), 1084-1087.
7. Altun, M.; Kramer, H. B.; Willems, L. I.; McDermott, J. L.; Leach, C. A.; Goldenberg, S. J.; Kumar, K. G.; Konietzny, R.; Fischer, R.; Kogan, E.; Mackeen, M. M.; McGouran, J.; Khoronenkova, S. V.; Parsons, J. L.; Dianov, G. L.; Nicholson, B.; Kessler, B. M., Activity-based chemical proteomics

accelerates inhibitor development for deubiquitylating enzymes. *Chemistry & biology* **2011**, 18 (11), 1401-12.

8. Ward, J. A.; McLellan, L.; Stockley, M.; Gibson, K. R.; Whitlock, G. A.; Knights, C.; Harrigan, J. A.; Jacq, X.; Tate, E. W., Quantitative Chemical Proteomic Profiling of Ubiquitin Specific Proteases in Intact Cancer Cells. *ACS Chem Biol* **2016**, 11 (12), 3268-3272.

9. Hewings, D. S.; Flygare, J. A.; Bogyo, M.; Wertz, I. E., Activity-based probes for the ubiquitin conjugation-deconjugation machinery: new chemistries, new tools, and new insights. *The FEBS Journal* **2017**, 284 (10), 1555-1576.

10. Lamberto, I.; Liu, X.; Seo, H. S.; Schauer, N. J.; Iacob, R. E.; Hu, W.; Das, D.; Mikhailova, T.; Weisberg, E. L.; Engen, J. R.; Anderson, K. C.; Chauhan, D.; Dhe-Paganon, S.; Buhrlage, S. J., Structure-Guided Development of a Potent and Selective Non-covalent Active-Site Inhibitor of USP7. *Cell chemical biology* **2017**, 24 (12), 1490-1500 e11.

11. D'Arcy, P.; Brnjic, S.; Olofsson, M. H.; Fryknas, M.; Lindsten, K.; De Cesare, M.; Perego, P.; Sadeghi, B.; Hassan, M.; Larsson, R.; Linder, S., Inhibition of proteasome deubiquitinating activity as a new cancer therapy. *Nat Med* **2011**, 17 (12), 1636-40.

12. Tian, Z.; D'Arcy, P.; Wang, X.; Ray, A.; Tai, Y. T.; Hu, Y.; Carrasco, R. D.; Richardson, P.; Linder, S.; Chauhan, D.; Anderson, K. C., A novel small molecule inhibitor of deubiquitylating enzyme USP14 and UCHL5 induces apoptosis in multiple myeloma and overcomes bortezomib resistance. *Blood* **2014**, 123 (5), 706-16.

13. de Jong, A.; Merckx, R.; Berlin, I.; Rodenko, B.; Wijdeven, R. H.; El Atmioui, D.; Yalcin, Z.; Robson, C. N.; Neefjes, J. J.; Ovaa, H., Ubiquitin-based probes prepared by total synthesis to profile the activity of deubiquitinating enzymes. *Chembiochem : a European journal of chemical biology* **2012**, 13 (15), 2251-8.

14. Kapuria, V.; Peterson, L. F.; Showalter, H. D.; Kirchhoff, P. D.; Talpaz, M.; Donato, N. J., Protein cross-linking as a novel mechanism of action of a ubiquitin-activating enzyme inhibitor with anti-tumor activity. *Biochemical pharmacology* **2011**, 82 (4), 341-9.

15. D'Arcy, P.; Linder, S., Proteasome deubiquitinases as novel targets for cancer therapy. *Int.J.Biochem.Cell Biol.* **2012**, 44 (11), 1729-1738.

16. Zhou, B.; Zuo, Y.; Li, B.; Wang, H.; Liu, H.; Wang, X.; Qiu, X.; Hu, Y.; Wen, S.; Du, J.; Bu, X., Deubiquitinase inhibition of 19S regulatory particles by 4-arylidene curcumin analog AC17 causes NF-kappaB inhibition and p53 reactivation in human lung cancer cells. *Molecular cancer therapeutics* **2013**, 12 (8), 1381-92.

17. Issaenko, O. A.; Amerik, A. Y., Chalcone-based small-molecule inhibitors attenuate malignant phenotype via targeting deubiquitinating enzymes. *Cell Cycle* **2012**, 11 (9), 1804-17.

18. Mullally, J. E.; Fitzpatrick, F. A., Pharmacophore model for novel inhibitors of ubiquitin isopeptidases that induce p53-independent cell death. *Molecular pharmacology* **2002**, 62 (2), 351-8.

19. Pinto, A.; Mace, Y.; Drouet, F.; Bony, E.; Boidot, R.; Draoui, N.; Lobysheva, I.; Corbet, C.; Polet, F.; Martherus, R.; Deraedt, Q.; Rodríguez, J.; Lamy, C.; Schicke, O.; Delvaux, D.; Louis, C.; Kiss, R.; Kriegsheim, A. V.; Dessy, C.; Elias, B.; Quetin-Leclercq, J.; Riant, O.; Feron, O., A new ER-specific photosensitizer unravels 1O₂-driven protein oxidation and inhibition of deubiquitinases as a generic mechanism for cancer PDT. *Oncogene* **2015**, 35, 3976.

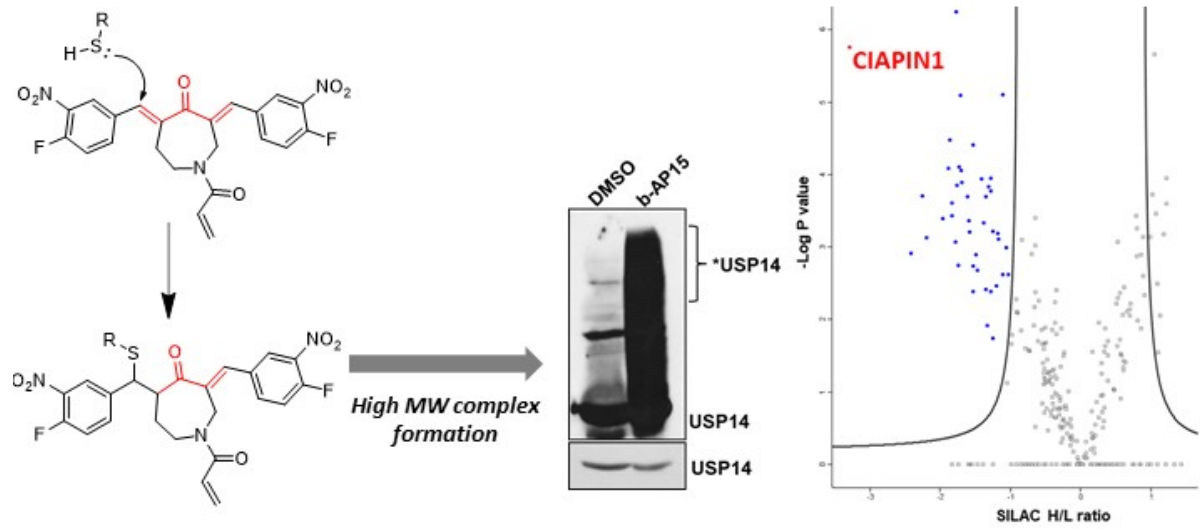
20. Wang, X.; D'Arcy, P.; Caulfield, T. R.; Paulus, A.; Chitta, K.; Mohanty, C.; Gullbo, J.; Chanan-Khan, A.; Linder, S., Synthesis and evaluation of derivatives of the proteasome deubiquitinase inhibitor b-AP15. *Chem Biol Drug Des* **2015**, 86 (5), 1036-48.

21. Wang, X.; Mazurkiewicz, M.; Hillert, E. K.; Olofsson, M. H.; Pierrou, S.; Hillertz, P.; Gullbo, J.; Selvaraju, K.; Paulus, A.; Akhtar, S.; Bossler, F.; Khan, A. C.; Linder, S.; D'Arcy, P., The proteasome deubiquitinase inhibitor VLX1570 shows selectivity for ubiquitin-specific protease-14 and induces apoptosis of multiple myeloma cells. *Sci Rep* **2016**, 6, 26979.

22. Borodovsky, A.; Ovaa, H.; Kolli, N.; Gan-Erdene, T.; Wilkinson, K. D.; Ploegh, H. L.; Kessler, B. M., Chemistry-based functional proteomics reveals novel members of the deubiquitinating enzyme family. *Chem Biol* **2002**, 9 (10), 1149-59.

23. Weerapana, E.; Simon, G. M.; Cravatt, B. F., Disparate proteome reactivity profiles of carbon electrophiles. *Nat Chem Biol* **2008**, 4 (7), 405-7.
24. Heal, W. P.; Jovanovic, B.; Bessin, S.; Wright, M. H.; Magee, A. I.; Tate, E. W., Bioorthogonal chemical tagging of protein cholesterylation in living cells. *Chem Commun (Camb)* **2011**, 47 (14), 4081-3.
25. Geiger, T.; Wisniewski, J. R.; Cox, J.; Zanivan, S.; Kruger, M.; Ishihama, Y.; Mann, M., Use of stable isotope labeling by amino acids in cell culture as a spike-in standard in quantitative proteomics. *Nat Protoc* **2011**, 6 (2), 147-57.
26. Sadaghiani, A. M.; Verhelst, S. H.; Bogoy, M., Tagging and detection strategies for activity-based proteomics. *Curr Opin Chem Biol* **2007**, 11 (1), 20-8.
27. Banci, L.; Bertini, I.; Calderone, V.; Ciofi-Baffoni, S.; Giachetti, A.; Jaiswal, D.; Mikolajczyk, M.; Piccioli, M.; Winkelman, J., Molecular view of an electron transfer process essential for iron-sulfur protein biogenesis. *Proceedings of the National Academy of Sciences* **2013**, 110 (18), 7136.
28. Song, G.; Cheng, C.; Li, Y.; Shaw, N.; Xiao, Z. C.; Liu, Z. J., Crystal structure of the N-terminal methyltransferase-like domain of anamorsin. *Proteins* **2014**, 82 (6), 1066-71.
29. Shibayama, H.; Takai, E.; Matsumura, I.; Kouno, M.; Morii, E.; Kitamura, Y.; Takeda, J.; Kanakura, Y., Identification of a Cytokine-induced Antiapoptotic Molecule Anamorsin Essential for Definitive Hematopoiesis. *The Journal of Experimental Medicine* **2004**, 199 (4), 581.
30. Wang, J.; Li, Q.; Wang, C.; Xiong, Q.; Lin, Y.; Sun, Q.; Jin, H.; Yang, F.; Ren, X.; Pang, T., Knock-down of CIAPIN1 sensitizes K562 chronic myeloid leukemia cells to Imatinib by regulation of cell cycle and apoptosis-associated members via NF-kappaB and ERK5 signaling pathway. *Biochem Pharmacol* **2016**, 99, 132-45.
31. Li, X.; Pan, Y.; Fan, R.; Jin, H.; Han, S.; Liu, J.; Wu, K.; Fan, D., Adenovirus-delivered CIAPIN1 small interfering RNA inhibits HCC growth in vitro and in vivo. *Carcinogenesis* **2008**, 29 (8), 1587-93.
32. Zhao, Y.; Wei Eric, W.; Qian, Z., CIAPIN1 siRNA Inhibits Proliferation, Migration and Promotes Apoptosis of VSMCs by Regulating Bcl-2 and Bax. *Current Neurovascular Research* **2013**, 10 (1), 4-10.
33. Zhang, Y.; Fang, J.; Ma, H., Inhibition of miR-182-5p protects cardiomyocytes from hypoxia-induced apoptosis by targeting CIAPIN1. *Biochem Cell Biol* **2018**, 96 (5), 646-654.
34. Lin, A.; Giuliano, C. J.; Palladino, A.; John, K. M.; Abramowicz, C.; Yuan, M. L.; Sausville, E. L.; Lukow, D. A.; Liu, L.; Chait, A. R.; Galluzzo, Z. C.; Tucker, C.; Sheltzer, J. M., Off-target toxicity is a common mechanism of action of cancer drugs undergoing clinical trials. *Sci Transl Med* **2019**, 11 (509).
35. Perez-Riverol, Y.; Csordas, A.; Bai, J.; Bernal-Llinares, M.; Hewapathirana, S.; Kundu, D. J.; Inuganti, A.; Griss, J.; Mayer, G.; Eisenacher, M.; Perez, E.; Uszkoreit, J.; Pfeuffer, J.; Sachsenberg, T.; Yilmaz, S.; Tiwary, S.; Cox, J.; Audain, E.; Walzer, M.; Jarnuczak, A. F.; Ternent, T.; Brazma, A.; Vizcaino, J. A., The PRIDE database and related tools and resources in 2019: improving support for quantification data. *Nucleic Acids Res* **2019**, 47 (D1), D442-D450.

TOC



VLX_Manuscript_Submission.docx (479.54 KiB)

[view on ChemRxiv](#) • [download file](#)

Supporting information

Re-evaluating the mechanism of action of α,β -unsaturated carbonyl DUB inhibitors b-AP15 and VLX1570: a paradigmatic example of unspecific protein crosslinking with Michael acceptor motif-containing drugs.

Jennifer A. Ward,^{1,2,5*} Adan Pinto-Fernandez,^{2,4*} Loïc Cornelissen,³ Sarah Bonham,² Laura Díaz-Sáez,^{1,2} Olivier Riant,⁴ Kilian V. M. Huber,^{1,2} Benedikt M. Kessler,² Olivier Feron,³ and Edward W. Tate⁵

¹Structural Genomics Consortium, Nuffield Department of Medicine, University of Oxford, Oxford, UK.

²Target Discovery Institute, Nuffield Department of Medicine, University of Oxford, Oxford, UK.

³Institute of Condensed Matter and Nanosciences Molecules, Solids and Reactivity (IMCN/MOST), UCLouvain, Brussels, Belgium.

⁴Pole of Pharmacology and Therapeutics (FATH), Institut de Recherche Expérimentale et Clinique (IREC), UCLouvain, Brussels, Belgium.

⁵Department of Chemistry, Imperial College London, Molecular Sciences Research Hub, White City Campus, London, UK.

*Corresponding authors: jennifer.ward@ndm.ox.ac.uk and adan.pintofernandez@ndm.ox.ac.uk

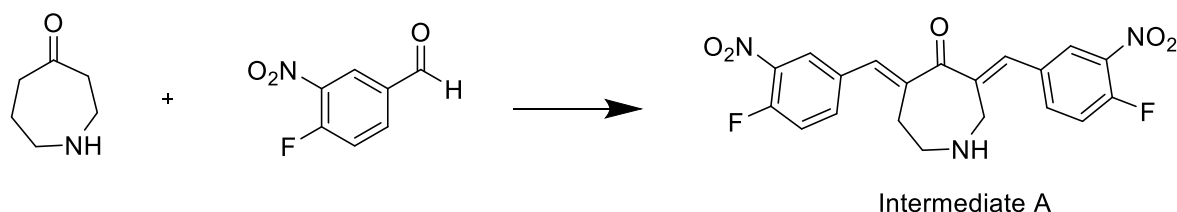
Supplementary methods

Reagents

Reagents were purchased from Sigma-Aldrich unless otherwise stated and used without further purification. b-AP15 and VLX1570 were purchased from Selleckchem and used as supplied without further purification. NeutrAvidin agarose resin and Dynabeads®MyOne™ Streptavidin C1 were purchased from Thermo Scientific. AzTB was synthesised as previously reported.¹

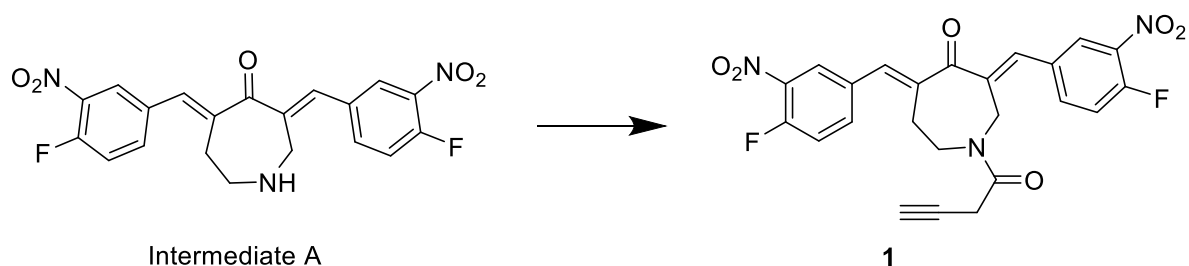
Primary antibodies: anti-Ub (Cell Signaling; catalogue number 3936) anti-USP14 (Cell Signaling; catalogue number 11931), anti-UCH-37 (Abcam; catalogue number ab124931) anti-USP28 (ABCAM, ab126604), anti-HA (12CA5) (Roche, 11583816001), anti-CIAPIN1 (Bethyl, A302-809A), anti-H3 (Cell signalling, 14269), anti-Actin (SantaCruz, sc-47778).

Synthesis of intermediate A



To a solution of 4-perhydroazepinone hydrochloride (500 mg, 34 mmol, 1 eq) and 4-fluoro-3-nitrobenzaldehyde (1.7 g, 101 mmol, 3 eq) in acetic acid (50 mL), H₂SO₄ (10 mL) was added dropwise at room temperature. After stirring for 48 hours, more H₂SO₄ (5 mL) was added. After a further 72 hours, additional 4-fluoro-3-nitrobenzaldehyde (600 mg, 101 mmol, 1.06 eq) was added. After a further 48 hours the reaction was deemed complete by LCMS analysis. The solution was diluted into 200 mL H₂O and extracted with EtOAc (2 × 150 mL). The combined layers were washed with brine (100 mL), dried over Na₂SO₄, and concentrated *in vacuo*. Crude **intermediate A** (1.4 g) was carried forward without purification. LCMS 416 [M+H]⁺

Synthesis of Compound 1



To a solution of **intermediate A** (280 mg, 0.67 mmol, 1 eq) and 3-butynoic acid (57 mg, 0.67 mmol, 1 eq) in THF (8 mL) at 0 °C, triethylamine (188 μ L, 135 mmol, 2 eq) was added, followed by dropwise addition of propylphosphonic anhydride (640 μ L, 101 mmol, 1.5 eq) as a 50% solution in EtOAc. The reaction was stirred at room temperature for 2 hours. The reaction was then diluted with 75 mL sat. NaHCO₃ and extracted with ethyl acetate (2 × 75 mL). The combined layers were washed with brine (100 mL), dried over Na₂SO₄, and concentrated *in vacuo*. The compound was purified by preparative

LC-MS. A 15 minute gradient of 15-80% Buffer B in Buffer A was used (Buffer A: acetonitrile/water = 5/95 with 20 mM ammonium acetate buffer, pH 6.0, Buffer B: acetonitrile/water = 80/20 with 20 mM ammonium acetate buffer, pH 6.0) to provide compound **1** as a yellow solid (13 mg, 4%). LCMS: ES- 480 [M-H]⁻, RT = 1.67, ¹H NMR (400 MHz, DMSO-*d*₆) δ 8.36 – 8.19 (m, 2H), 8.05 – 7.88 (m, 2H), 7.76 – 7.54 (m, 3H), 7.51 – 7.36 (m, 1H), 6.50-5.80 (m, 1H), 5.36 – 5.11 (m, 2H), 4.99 – 4.85 (m, 1H), 4.85 – 4.65 (m, 1H), 3.90 – 3.74 (m, 2H), 3.22-2.92 (m, 2H).

Cell culture

Cells were cultured at 37 °C in a humidified 5% CO₂ atmosphere in media (DMEM for HeLa, U2OS, and SiHa; RPMI for KMS11 and HCT116; EGM-2 for HUVECS) containing 10% FBS. Cells were grown until approximately 80% confluent before treatment with indicated concentrations of compounds or DMSO control.

Immunoblot analysis

Cells were washed with ice-cold PBS and lysed with RIPA buffer containing protease and phosphatase inhibitors. Proteins coming from either treated cells or treated cell extracts were separated by SDS-PAGE and detected with the indicated antibodies.

Ub-AML DUB activity Assay

DUB activities were measured using dedicated Glo Cell-Based Reagents and a Glomax microplate reader (Promega) following the manufacturer's instructions; for the DUB assay, Ub-AML (Boston Biochem, Cambridge, MA, USA) was used as a substrate. Activities of recombinant DUBs (purchased from Boston Biochem) or HeLa crude extracts (prepared as for ABP assays) were measured using this protocol.

Ha-UB-C2Br DUB ABP labelling assays

HA-Ub-C2Br was synthesised in the Kessler lab ² and ABP assays were performed as previously described. ³ Briefly, Crude HeLa cell extracts were pre-incubated with DMSO (vehicle), b-AP15 (200 μM) and NEM (200 μM) for 30 minutes at 37°C, labeled with HAUbC2Br for 45 min at 37°C, separated in 4-15% SDS-PAGE gradient gels and immunoblotted with specific anti-USP28 antibody.

Compound 1 ABPP labelling assay

Cells were pre-incubated with indicated concentrations of VLX1570 or b-AP15 for 30 min before treatment with **1** for 1 hour. Cells were then lysed in Buffer C (1% v/v Triton X-100, 0.1% w/v SDS, 1x EDTA-free complete protease inhibitor (Roche Diagnostics) in PBS), protein concentrations were determined, and the lysates stored at -80 °C until use. Samples were analysed by in-gel fluorescent analysis following CuAAC ligation (see below).

CuAAC ligation

A premixed click cocktail (100 μ M AzTb, 10 mM CuSO₄, 10 mM TCEP and 100 μ M TBTA, final concentrations) was added to lysate adjusted to a final protein concentration of 1 mg/mL. The samples were vortexed for 1 h at room temperature and then quenched with 5 mM EDTA. Protein was precipitated by sequential addition of MeOH (2 \times volumes), CHCl₃ (0.5 \times volume) and H₂O (1 \times volume). Protein was pelleted (17,000 \times g, 5 min) washed with MeOH (10 \times volumes) and re-pelleted.

In-gel fluorescence

Pellets were air dried and suspended in PBS buffer containing 2% w/v SDS. 4 \times sample loading buffer (NuPAGE LDS sample buffer) containing 4% v/v β -mercaptoethanol was then added and samples heated for 6 min at 90 °C. Samples were separated by SDS-PAGE and the gels scanned using a Typhoon FLA 9500 Imager (GE Healthcare) equipped with 532 nm laser and LPG filter to visualise both the TAMRA fluorophore and molecular weight markers (Precision Plus All Blue Standards, Bio-Rad).

SILAC Cell Culture and Spike-in SILAC quantification

U2OS cells were cultured as previously described or in ¹⁵N₄ ¹³C₆-arginine and ¹⁵N₂ ¹³C₆-lysine (R10K8) containing DMEM media (Dundee Cell) with 10% v/v dialysed FBS. Cells grown in unlabelled media were treated in triplicate for 1 h with 5 μ M of **1** after a 30 min pre-incubation with a fixed concentration of VLX1570 (0, 5 μ M, 20 μ M). In parallel, R10K8 incorporated U2OS cells were treated with 5 μ M of **1** for 1 h to generate the 'spike-in' standard. Both spike and treatment cells were lysed in Buffer C, and stored at -80 °C until use.

Sample Preparation for Proteomic analysis

Sample preparation was conducted as previously described.⁴ Briefly, 400 μ g of each competition condition was mixed with 200 μ g of spike, the protein concentration adjusted to 2 mg/mL, and CuAAC ligation performed. Protein pellets were resuspended in 0.2 % w/v SDS, 1 mM dithiothreitol in PBS to give a final protein concentration of 1 mg/mL. Samples were enriched on NeutrAvidin agarose resin (30 μ L, pre-washed three times in 0.2% w/v SDS in PBS) by incubation with gentle shaking for 2 h at room temperature. The supernatant was then removed, and the beads washed consecutively with: 3 \times 1% w/v SDS in PBS, 2 \times 4M Urea in PBS, 5 \times 50 mM ammonium bicarbonate (AMBIC). The washed beads were resuspended in 50 μ L of 50 mM AMBIC and reduced with 10 mM dithiothreitol at 55 °C for 30 min. The samples were washed twice and resuspended in 50 μ L of 50 mM AMBIC, and cysteines were alkylated by 10 mM iodoacetamide in the dark for 30 min. The samples were washed twice and resuspended in 50 μ L of 50 mM AMBIC, treated with trypsin (5 μ L, 0.2 mg / ml, Promega) and digested overnight at 37 °C. The supernatant was retained and the beads washed with 80 μ L AMBIC followed by 80 μ L 0.1% v/v TFA in H₂O (80 μ L). The combined supernatants were desalted and dried in vacuo. Dried peptides were stored at -80 °C, and resuspended in 0.5% v/v TFA, 2% v/v MEQH in H₂O (20 μ L) for LC-MS/MS analysis.

ABPP LC-MS/MS data acquisition

LC-MS/MS runs were performed at Imperial College London on an Easy nLC-1000 system coupled to a QExactive mass spectrometer via an easy-spray source (all Thermo Fisher Scientific). 3 μ L injections of peptide sample were separated on a reverse phase Acclaim PepMap RSLC column (50 cm x 75 μ m inner diameter, Thermo Fisher Scientific) across a 2 h acetonitrile gradient containing 0.1 % v/v formic acid, using a flow rate of 250 nL/min. The instrument was operated in a data-dependent cycling mode with survey scans acquired at a resolution of 75,000 at m/z 200 (transient time 256 ms). The top 10 most abundant isotope patterns with charge +2 from this survey scan were then selected with an isolation window of 3.0 m/z and subjected to MS/MS fragmentation by HCD with normalized collision energies of 25. The maximum ion injection times for the survey scan and the MS/MS scans were 250 and 80 ms, respectively. The ion target value for MS was set to 106 and for MS/MS to 105, and the intensity threshold was set to 8.3×10^2 .

ABPP Data analysis

The raw data was processed using MaxQuant version 1.5.0.253 and the reference complete human proteome FASTA file. 'Arg10' and 'Lys8' were selected as heavy labels, cysteine carbamidomethylation was selected as a fixed modification, and methionine oxidation as a variable modification. Default settings for identification and quantification were used. Specifically, a minimum peptide length of 7, a maximum of 2 missed cleavage sites, and a maximum of 3 labelled amino acids per peptide were employed. Peptides and proteins were identified utilising a 0.01 false discovery rate, with "Unique and razor peptides" mode selected for both identification and quantification of proteins (razor peptides are uniquely assigned to protein groups and not to individual proteins). At least 2 razor + unique peptides were required for valid quantification. Processed data was further analysed using Perseus version 1.5.0.9 and Microsoft Excel 2010. Peptides categorised by MaxQuant as 'potential contaminants', 'only identified by site' or 'reverse' were filtered, and the processed H/L ratios transformed in Log₂(L/H) ratios. The ratios for each experimental condition were normalised relative to their median, and biological triplicates grouped. The detection of at least 2 unique peptides was used as a threshold for protein identification and 2 valid ratio values were required in at least one experimental group for quantification. Statistically significant competition was determined through the application of a P2 test, using a permutation-based FDR of 0.01 and an S0 of 0.1. To determine the relative response to inhibition, the average fold change was calculated for each protein under each inhibitor condition, by normalising all mean ratios relative to the condition lacking inhibitor (0 μ M compound 1).

GO term analysis of the 24 targets significantly competed by both 5 and 20 μ M VLX1570 was conducted in STRING (<http://string-db.org>). Basic STRING settings were used for protein interaction network generation, with all active interaction sources (Textmining, Experiments, Databases, Co-expression, Neighborhood, Gene Fusion, Co-occurrence) considered. The observed Gene Ontology Cellular component (GO CC) enrichment of this network is summarised in **Supplementary Table 1**.

Cell viability assays

KMS11 cells were seeded at 25,000 cells/well (100 μ L) in a 96-well plate and treated with varying concentrations of VLX150 or compound 1. For U2OS cells, cells were seeded at 10,000 (100 μ L) in a 96-well plate and left overnight to adhere before continuing with the compound treatments

described above. DMSO and bortezomib (10 mM) were used as positive and negative controls and all experiments were set up in biological triplicates. Following a 72 hour incubation, CellTiter Glo reagent was added according to manufacturer's instructions (Promega) and luminescence measured. EC₅₀ values were determined by fitting the data to the IC₅₀ dose response function using GraphPad Prism 7.

To analyse the impact of glutathione (GSH) on compound potency, KMS11 cells were seeded at 80,000 cell/well (100 μ L) in a 96-well plate and treated with VLX1570 or b-AP15 (1 μ M or 10 μ M) with and without GSH present (1mM). DMSO was used as a control and all experiments were set up with 6 biological replicates. After 16 hours of incubation Alamar blue was added according to manufacturer's instructions (Thermo Scientific) with fluorescence measured at 560/590 nm excitation/emission. Cell viability was normalised to the DMSO control and the data plotted with Graphpad Prism 7.

siRNA studies

SMARTpool: ON-TARGETplus CIAPIN1 siRNA (Dharmacon, 4 μ L, 10 μ M stock solution) was added to 500 μ L Opti-MEM in a 6-well plate and mixed gently before lipofectamine RNAiMAX (Thermo Fisher, 4 μ L) was added. The mixture was incubated at room temperature for 20 minutes before addition of KMS11 cells (1.5 mL, 80,000 cells/mL) suspended in RPMI media. AllStars Negative Control siRNA (Qiagen) and water were used as scramble and vehicle controls, respectively, and all experiments were set up in biological triplicate. After 72 hours, 100 μ L of cell suspension was transferred into a 96-well plate and cell viability measured by CellTiter Glo as described above. The remaining cells were pelleted and lysed as described above for immunoblot analysis.

Protein expression and purification

CIAPIN1 encoding pQTEV-LOC57019 was a gift from Konrad Buessow (Addgene plasmid # 34811; <http://n2t.net/addgene:34811> ; RRID:Addgene_34811). pQTEV-LOC57019 was transformed into *E. coli* Rosetta cells. The cells were cultured in batch mode at 37 °C in the presence of 100 μ g/mL of ampicillin and 34 μ g/mL of chloroamphenicol in 100 mL TB (10 flasks in total) until an OD of 0.6 was reached. Batch mode was used, as degradation of the protein was observed under larger scale expression conditions. Induction was achieved with IPTG (200 μ M final concentration) and overnight incubation at 18 °C. The cells were harvested by centrifugation (4000 *g*, 30 minutes) and the resulting cell pellet lysed by sonication (15 sec on/off, 7.5 min) in 50 mL Buffer D (20 mM HEPES, 500 mM NaCl, 5% glycerol, 20 mM imidazole, 0.5% TCEP, pH 7.5) supplemented with Protease Inhibitor Cocktail Set III, EDTA-Free (Merck), and benzonase. The lysate was spun at 4000 *g* for 1 hour at 4 °C before the resulting supernatant was incubated for 45 minutes at 4 °C with HisPur™ Ni-NTA superflow agarose beads (10 mL, Thermo Scientific) that had been pre-equilibrated in Buffer D (3 x 30 mL). The beads were then washed (5 x 10 mL Buffer D) and purified protein eluted with 50 mL Buffer E (20 mM HEPES, 500 mM NaCl, 5% glycerol, 500 mM imidazole, 0.5% TCEP, pH 7.5). The eluted protein was concentrated and further purified by size exclusion chromatography using a HiLoad 16/600 Superdex S200 column (GE Healthcare) equilibrated with Buffer F (20 mM HEPES, 150 mM NaCl, pH 7.5). The resulting protein purity was assessed by SDS-PAGE, and protein identity was confirmed by tryptic digest analysis (96% coverage). Protein concentration was determined to be 7.6 mg/mL, and was calculated using a theoretical molar extinction coefficient of 13,980 M⁻¹cm⁻¹ as determined by ProtParam.⁵

SDS page and Size exclusion analysis

Recombinant CIAPIN1 (10 μ L, 1 mg/mL) was incubated with DMSO (0.16%) or VLX1570 at 1x, 2x, 5x, or 10x molar excess for 30 minutes at 4 °C before addition of sample loading buffer and analysis by SDS-PAGE.

For SEC analysis of aggregates, CIAPIN1 (100 μ L, 7.6 mg/mL) was incubated DMSO (0.16%) or 2X molar excess of VLX1570 for 30 minutes at 4 °C before loading onto a Superdex S200 10/30 GL column (GE Healthcare) equilibrated with Buffer F. Gel filtration standard (BioRad) was used to generate a standard curve.

Peptide mapping analysis

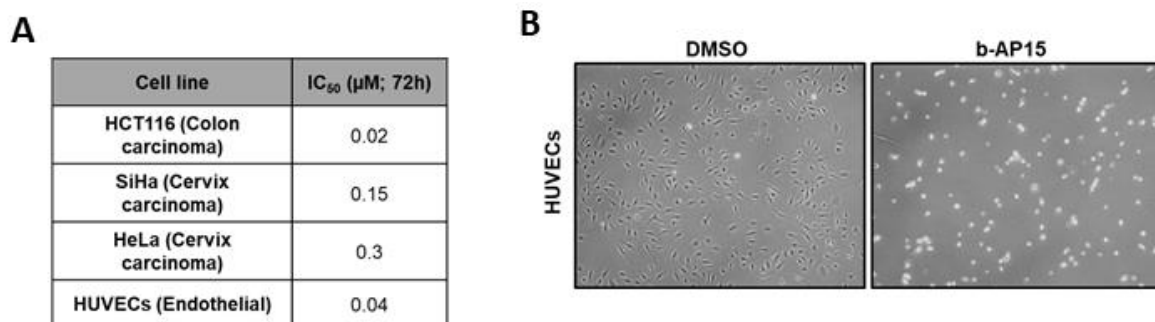
Recombinant CIAPIN1 (5 μ L, 1mg/mL) was incubated with DMSO (0.16%) or VLX1570 (10x molar excess) for 30 minutes at 4 °C before Trypsin (Promega V5111, 2 μ L; 20 μ g in 100 μ L Trypsin resuspension buffer) was added and the mixture incubated overnight at 37 °C. An aliquot of the digestion mixture (2 μ L) was taken and diluted in 0.1% v/v FA, 2% v/v acetonitrile in H₂O (30 μ L) for LC-MS/MS analysis. Mass spectrometry data were acquired at the Discovery Proteomics Facility (University of Oxford). LC MS/MS analysis was performed using a Dionex Ultimate 3000 nano-ultra high pressure reverse phase chromatography coupled on-line to a Q Exactive mass spectrometer (Thermo Scientific). Samples were desalted online (PepMAP C18, 300 μ m x 5mm, 5 μ m particle, Thermo) for 1 minute at a flow rate of 20 μ L/min and separated on an EASY-Spray PepMap RSLC C18 column (500 mm x 75 μ m, 2 μ m particle size, Thermo Scientific) over a 60 minute gradient of 2-35 % acetonitrile in 5 % DMSO, 0.1% formic acid at 250 nL/min. MS1 scans were acquired at a resolution of 70,000 at 200 m/z and the top 15 most abundant precursor ions were selected for HCD fragmentation.

MS data were processed with PEAKS software (v 8.5),⁶ searching against the UniprotKB Human database with protein of interest CIAPIN1 (Uniprot Q6FI81) included. Trypsin (specific, maximum 1 missed cleavage) was selected as the digestion enzyme. A mass tolerance of 10 ppm for precursor and 0.05 Da for fragment ions was used. Oxidation (M), Deamination (N, Q) and addition of VLX1570 (+469.11, single addition) were selected as variable modifications, and an FDR of 1% was applied for peptide matches.

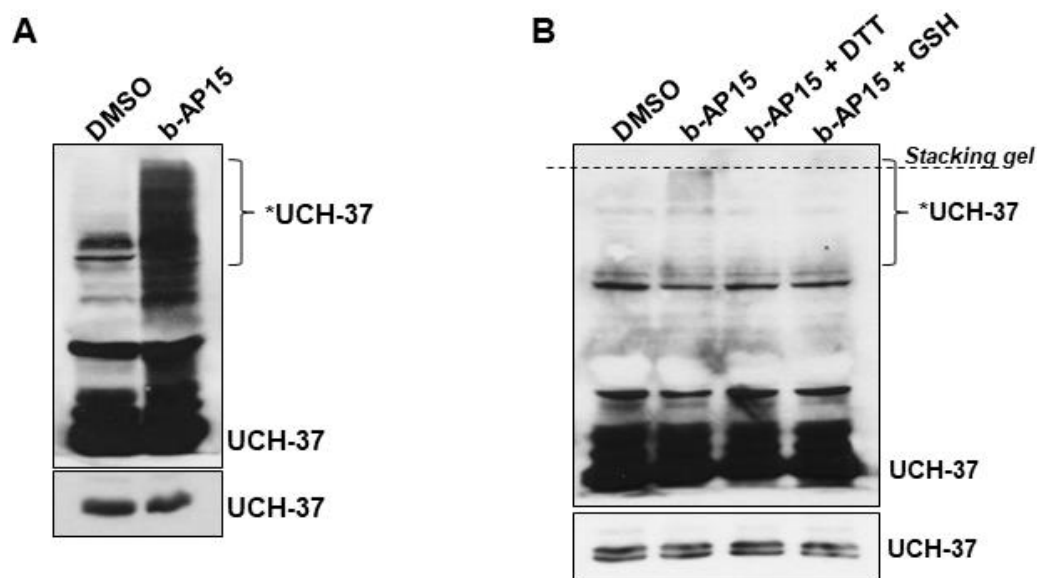
ES-MS analysis

His-tagged CIAPIN1 (full length human (AA1-312) with a C-terminal 7x His tag and TEV site (KHHHHHHHS DYDIPTTENL YFQGS, 36502.38 Da, 1 mg/mL, 27 μ M) was incubated with 2 molar equivalents of VLX1570 (54 μ M) in PBS for 10 minutes and analysed by ES-MS.

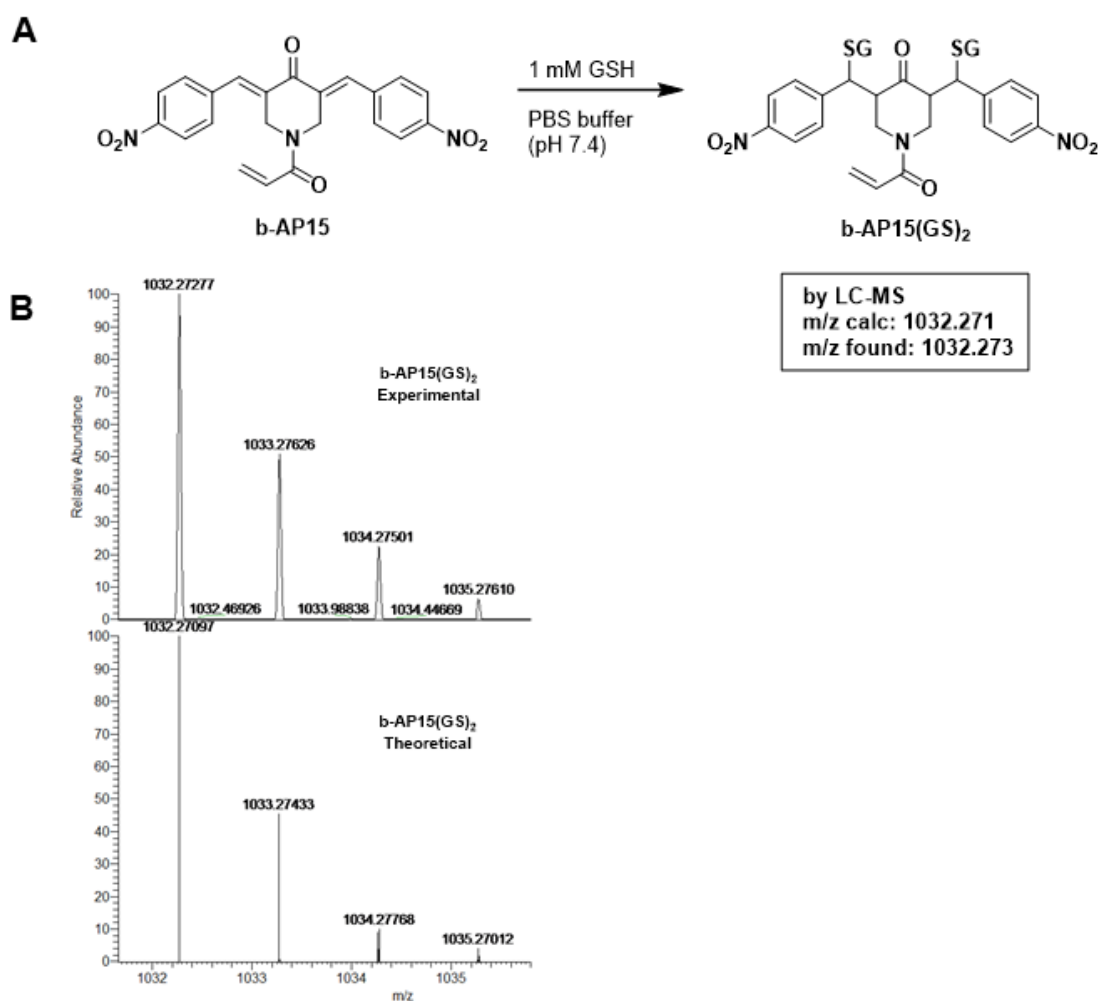
Supplementary Figures and Tables



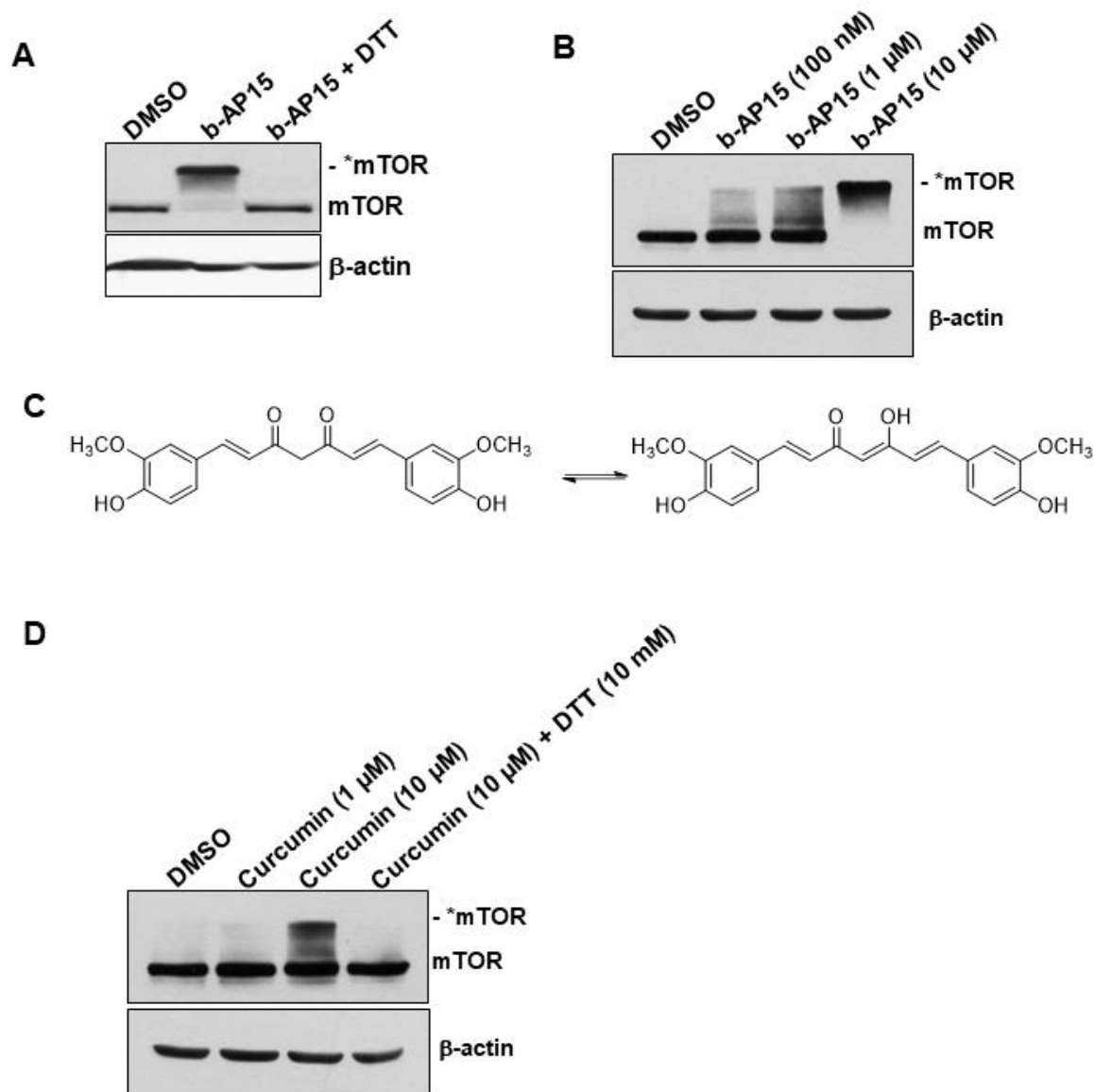
Supplementary Figure 1. (A) IC₅₀ values measured by the CellTiter Glo assay for tumor and endothelial cell lines exposed to b-AP15 for 72 h (n=6). **(B)** Representative microscope picture showing the toxic effects of b-AP15 (1 μM) on HUVECs cells after 18 hours of incubation.



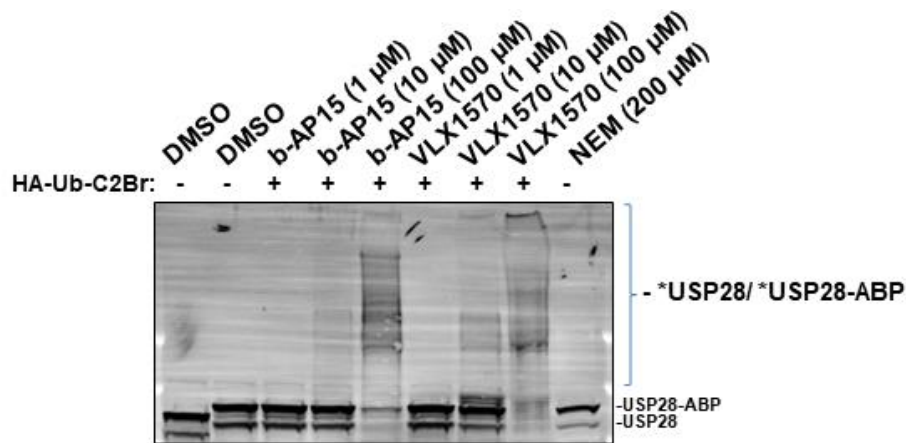
Supplementary Figure 2. Immunoblot analysis of high MW UCH-37 in **(A)** HeLa crude cell extracts incubated with b-AP15 (10 μM) for 2 hours at 37°C, and in **(B)** HeLa cells treated with either vehicle, 10 μM b-AP15 or with 10 μM b-AP15 in combination with reducing agents (10 mM dithiothreitol (DTT) or 10 mM glutathione (GSH)) for 2 hours.



Supplementary Figure 3. (A) Schematic of GSH addition to b-AP15 **(B)** Comparison of theoretical LC-MS peaks for b-AP15(GS)₂ with experimental peaks obtained on incubation of b-AP15 (10 μ M) in PBS with GSH (1 mM) for 1 hour.

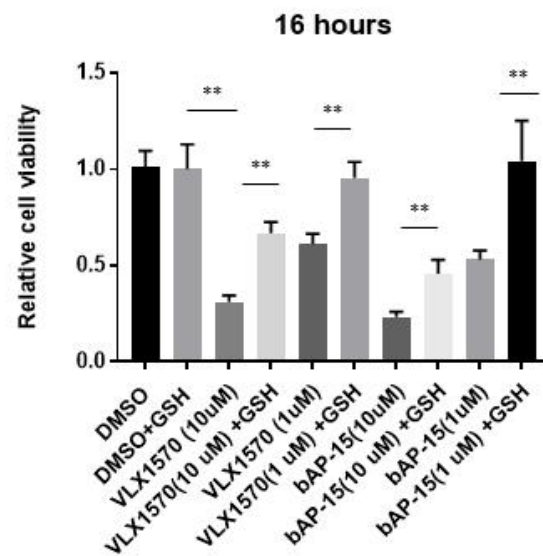


Supplementary Figure 4. Immunoblot analysis of high MW mTOR complex accumulation in **(A)** HeLa crude cell extracts incubated with b-AP15 (10 μ M) with or without reducing agent for 2 hours at 37°C and **(B)** in HeLa crude cell extracts incubated with increasing concentrations of b-AP15 (100 nM, 1 μ M and 10 μ M) for 1 hour at 37°C. **(C)** Molecular structure of curcumin. **(D)** Immunoblot analysis of high MW mTOR complex accumulation in HeLa crude cell extracts incubated with curcumin or vehicle (DMSO) for 1 hour at 37°C, following a 15 minute pre-treatment with either vehicle or DTT (10 mM).

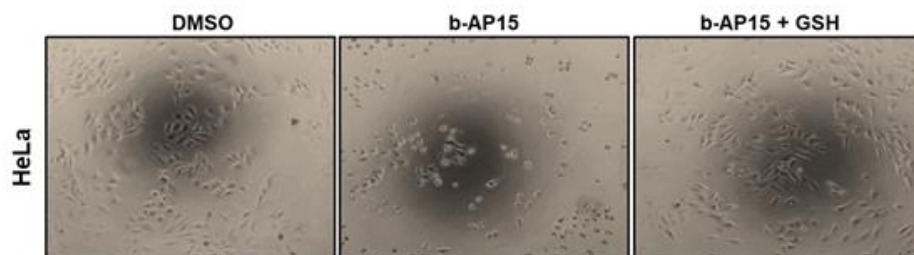


Supplementary Figure 5. Immunoblot analysis of high MW USP28 complex accumulation in crude HeLa cell extracts treated with DMSO, b-AP15, and NEM, for 30 minutes at 37°C and then labelled with HAUbC2Br.

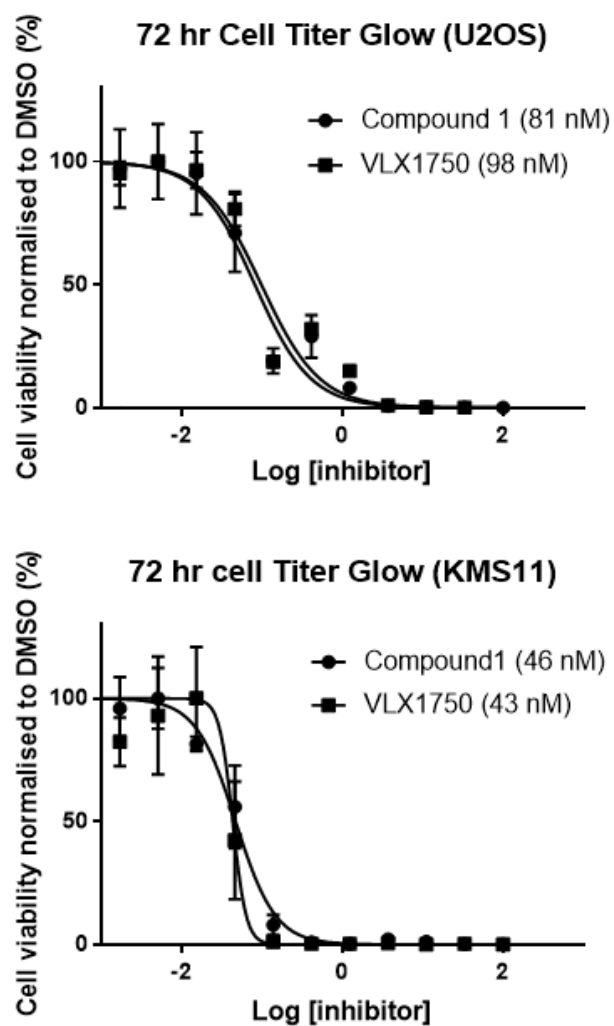
A



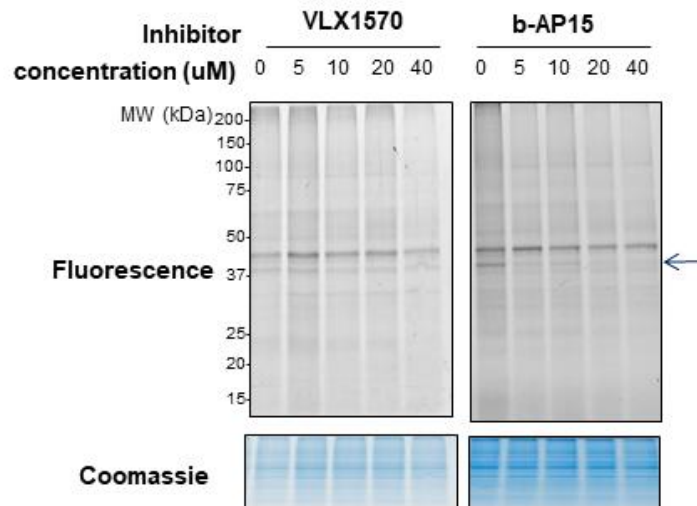
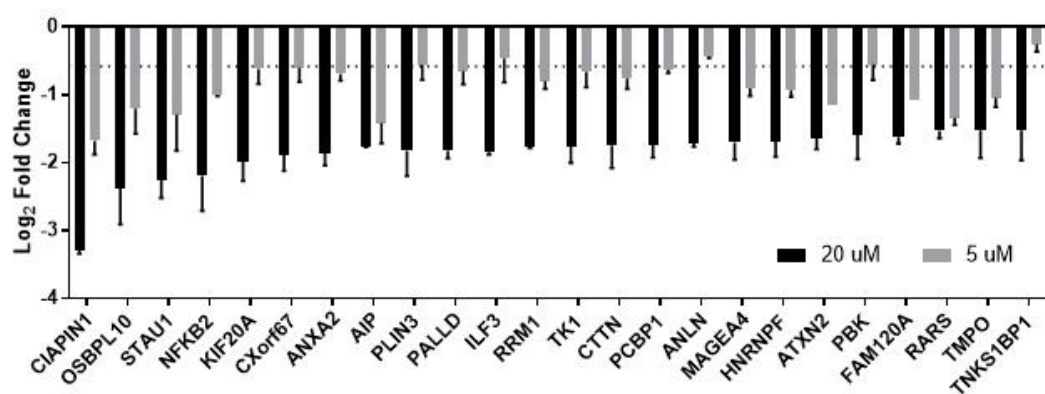
B



Supplementary Figure 6. (A) Alamar blue analysis of KMS11 cells incubated with compound with or without GSH (1 mM) for 16 hours **(B)** Representative microscope pictures of HeLa cells incubated with b-AP15 (10 μM) with or without reducing agents (10 mM) for 2 hours at 37°C.



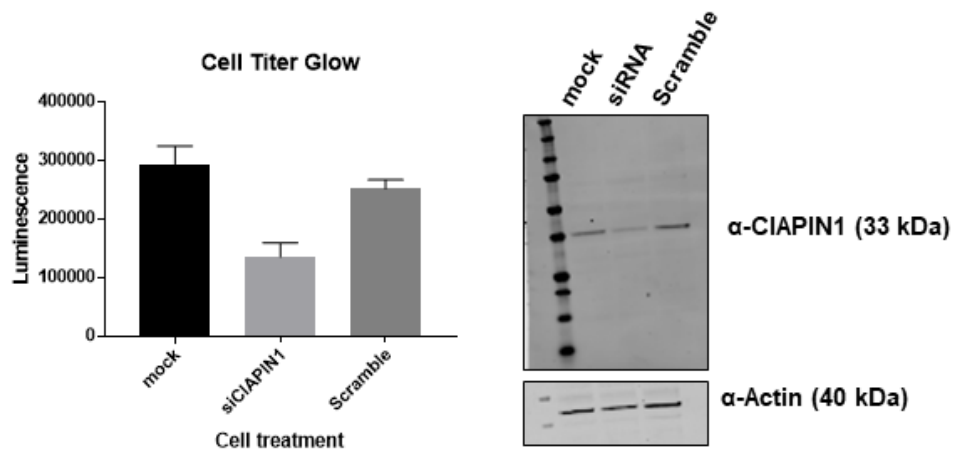
Supplementary Figure 7. CellTiter Glo experiment with VLX1570 and compound 1 demonstrates conserved cytotoxicity in U2OS and KMS11 cells. IC₅₀ values are given in parentheses.

A**B**

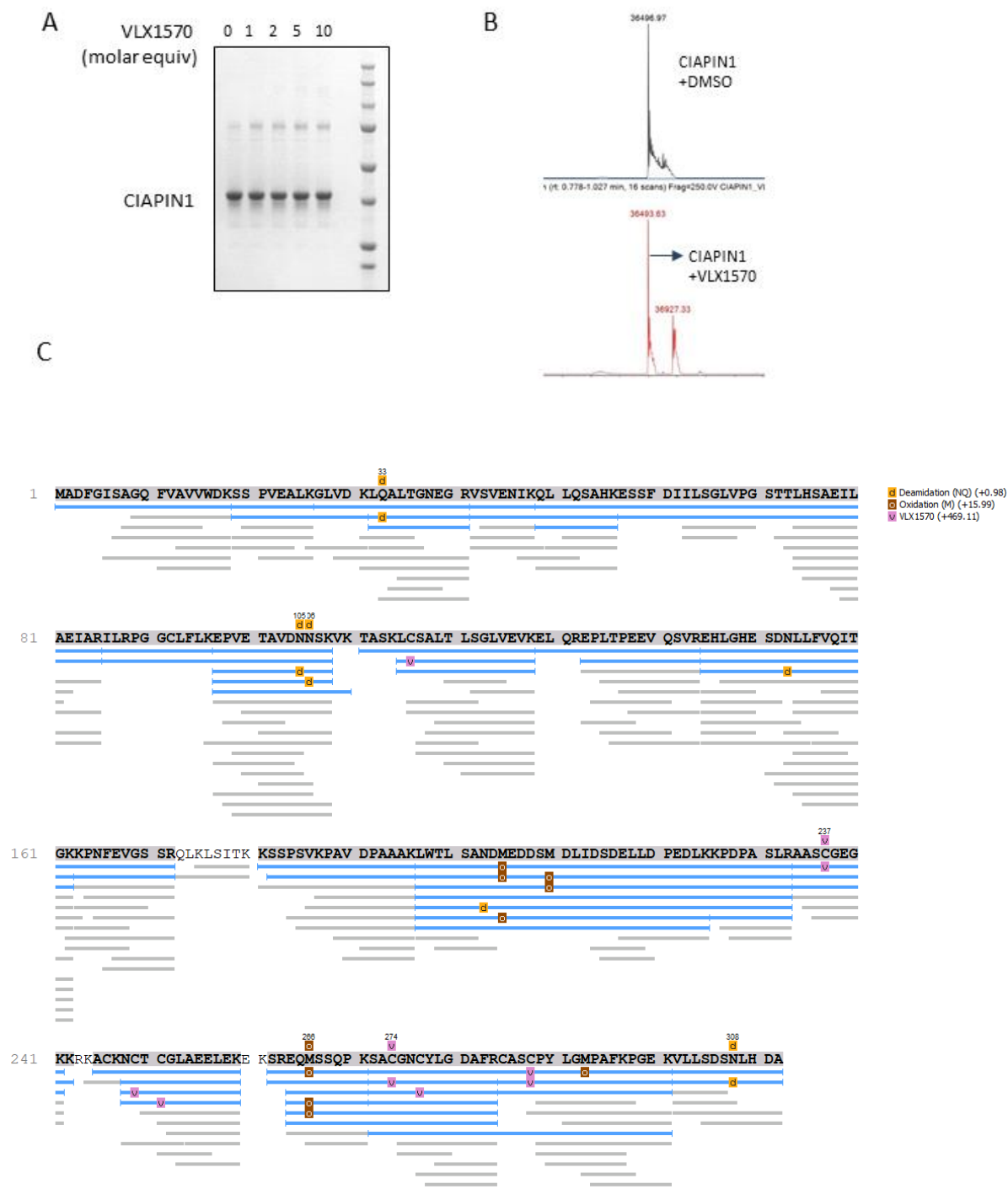
Supplementary Figure 8. (A) In-gel fluorescence analysis of compound **1** (5 μ M) labelled U2OS proteome in competition with VLX1570 and structurally related inhibitor bAP-15. **(B)** Targets of compound **1** (5 μ M) identified as being significantly competed (FDR=0.05, S_0 = 0.2) by VLX1570 (at both 20 μ M and 5 μ M). The dashed line indicates a 1.5 fold change.

Supplementary Table 1. Gene Ontology Cellular Component (GO CC) enrichment analysis of the 24 targets competed by both 5 and 20 μ M of VLX1570. Analysis was conducted using STRING software.

Pathway ID	pathway description	observed gene count	false discovery rate	matching proteins in your network (labels)
GO.0005829	cytosol	16	0.0053	AIP,ANXA2,ATXN2,CTTN,FAM120A,HNRNPF,NFKB2,OSBPL10,PALLD,PCBP1,PLIN3,RARS,RRM1,STAU1,TK1,TNKS1BP1
GO.0043232	intracellular non-membrane-bounded organelle	14	0.0059	ANLN,ANXA2,ATXN2,CIAPIN1,CTTN,ILF3,KIF20A,OSBPL10,PALLD,PCBP1,PLIN3,STAU1,TMPO,TNKS1BP1
GO.0002102	podosome	2	0.0207	CTTN,PALLD
GO.0032991	protein-containing complex	14	0.0207	AIP,ANXA2,ATXN2,CTTN,HNRNPF,ILF3,KIF20A,NFKB2,PALLD,PCBP1,RARS,RRM1,STAU1,TNKS1BP1
GO.0043231	intracellular membrane-bounded organelle	21	0.0207	AIP,ANLN,ANXA2,ATXN2,CIAPIN1,CTTN,CXorf67,FAM120A,HNRNPF,ILF3,KIF20A,NFKB2,PALLD,PBK,PCBP1,PLIN3,RARS,RRM1,STAU1,TMPO,TNKS1BP1
GO.0044428	nuclear part	13	0.0207	AIP,ANLN,CIAPIN1,CXorf67,HNRNPF,ILF3,KIF20A,NFKB2,PCBP1,RARS,RRM1,TMPO,TNKS1BP1
GO.0044444	cytoplasmic part	20	0.0207	AIP,ANLN,ANXA2,ATXN2,CIAPIN1,CTTN,FAM120A,HNRNPF,ILF3,KIF20A,NFKB2,OSBPL10,PALLD,PCBP1,PLIN3,RARS,RRM1,STAU1,TK1,TNKS1BP1
GO.0044446	intracellular organelle part	19	0.0207	AIP,ANLN,ANXA2,ATXN2,CIAPIN1,CTTN,CXorf67,HNRNPF,ILF3,KIF20A,NFKB2,PALLD,PCBP1,PLIN3,RARS,RRM1,STAU1,TMPO,TNKS1BP1
GO.0001726	ruffle	3	0.0232	ANXA2,CTTN,PALLD
GO.0030496	midbody	3	0.0232	ANLN,ANXA2,KIF20A
GO.0043229	intracellular organelle	22	0.0232	AIP,ANLN,ANXA2,ATXN2,CIAPIN1,CTTN,CXorf67,FAM120A,HNRNPF,ILF3,KIF20A,NFKB2,OSBPL10,PALLD,PBK,PCBP1,PLIN3,RARS,RRM1,STAU1,TMPO,TNKS1BP1
GO.0005634	nucleus	16	0.0255	AIP,ANLN,CIAPIN1,CXorf67,FAM120A,HNRNPF,ILF3,KIF20A,NFKB2,PALLD,PBK,PCBP1,RARS,RRM1,TMPO,TNKS1BP1
GO.0005737	cytoplasm	21	0.0255	AIP,ANLN,ANXA2,ATXN2,CIAPIN1,CTTN,FAM120A,HNRNPF,ILF3,KIF20A,NFKB2,OSBPL10,PALLD,PCBP1,PLIN3,RARS,RRM1,STAU1,TK1,TMPO,TNKS1BP1
GO.0010494	cytoplasmic stress granule	2	0.0255	ATXN2,STAU1
GO.0036464	cytoplasmic ribonucleoprotein granule	3	0.0255	ATXN2,PCBP1,STAU1
GO.1990904	ribonucleoprotein complex	5	0.0255	ATXN2,HNRNPF,ILF3,PCBP1,STAU1
GO.0005938	cell cortex	3	0.0262	ANLN,ANXA2,CTTN
GO.0032155	cell division site part	2	0.0262	ANLN,KIF20A
GO.0044424	intracellular part	23	0.0294	AIP,ANLN,ANXA2,ATXN2,CIAPIN1,CTTN,CXorf67,FAM120A,HNRNPF,ILF3,KIF20A,NFKB2,OSBPL10,PALLD,PBK,PCBP1,PLIN3,RARS,RRM1,STAU1,TK1,TMPO,TNKS1BP1
GO.0005811	lipid droplet	2	0.0321	ANXA2,PLIN3
GO.0030863	cortical cytoskeleton	2	0.0333	ANLN,CTTN
GO.0031981	nuclear lumen	11	0.0372	AIP,ANLN,CIAPIN1,CXorf67,HNRNPF,ILF3,KIF20A,NFKB2,PCBP1,RARS,TNKS1BP1
GO.0005654	nucleoplasm	10	0.0377	AIP,ANLN,CIAPIN1,CXorf67,HNRNPF,ILF3,KIF20A,NFKB2,PCBP1,RARS

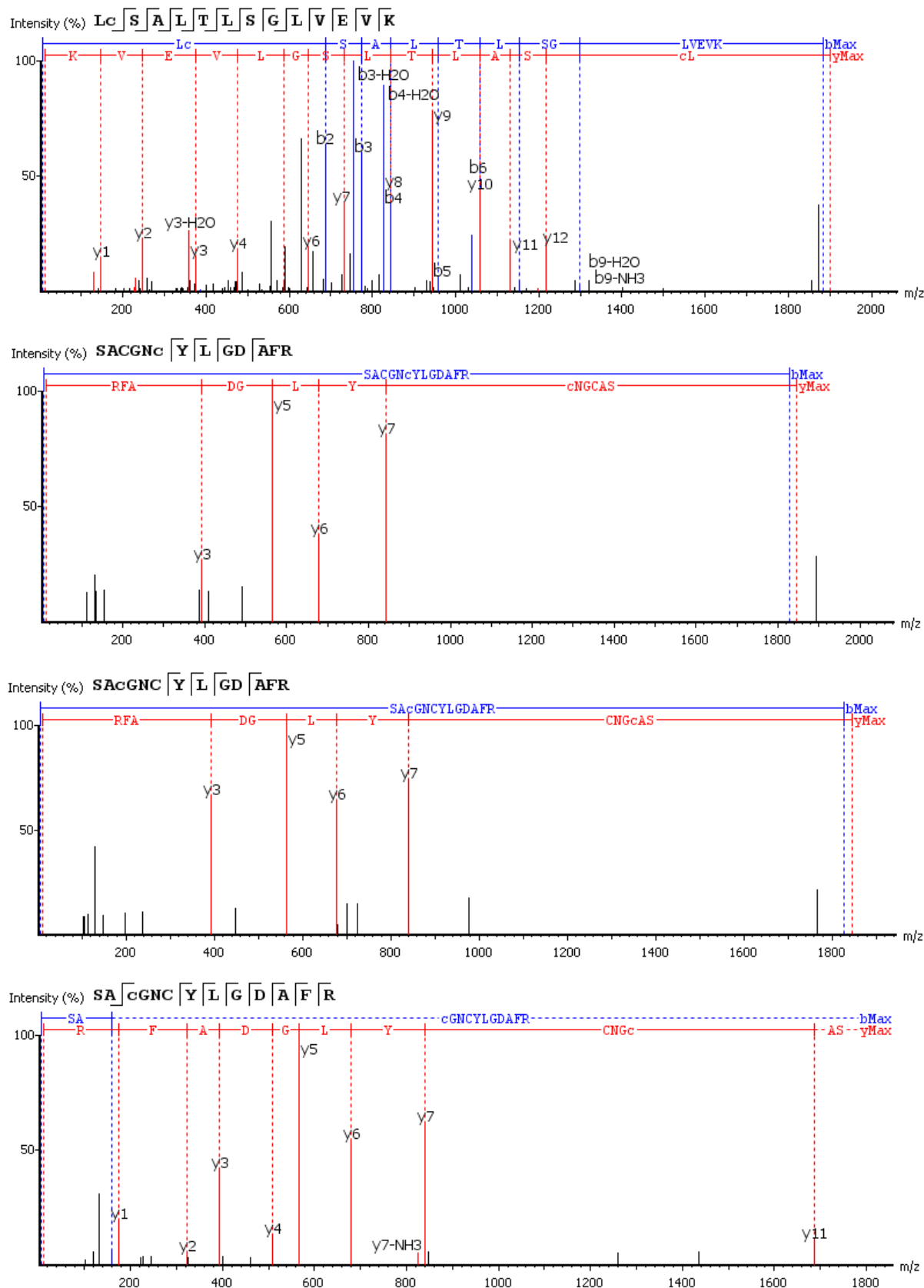


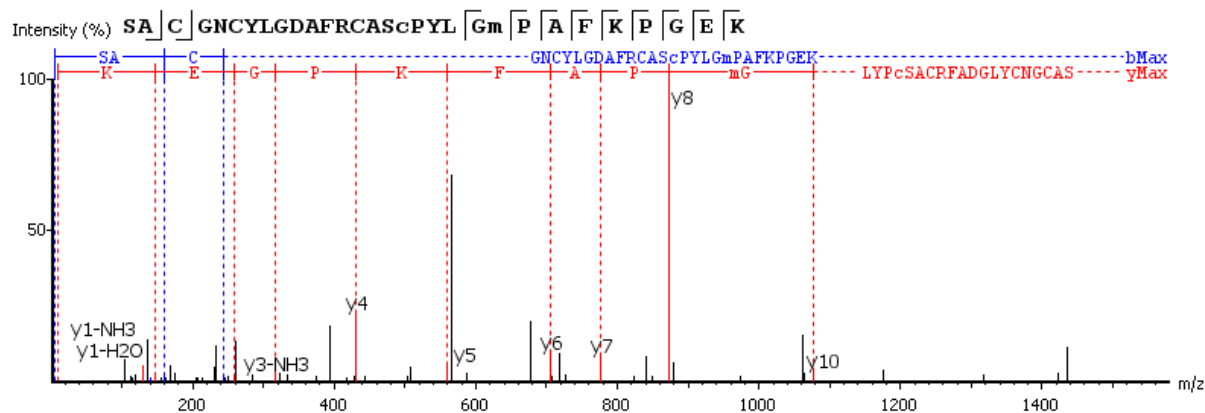
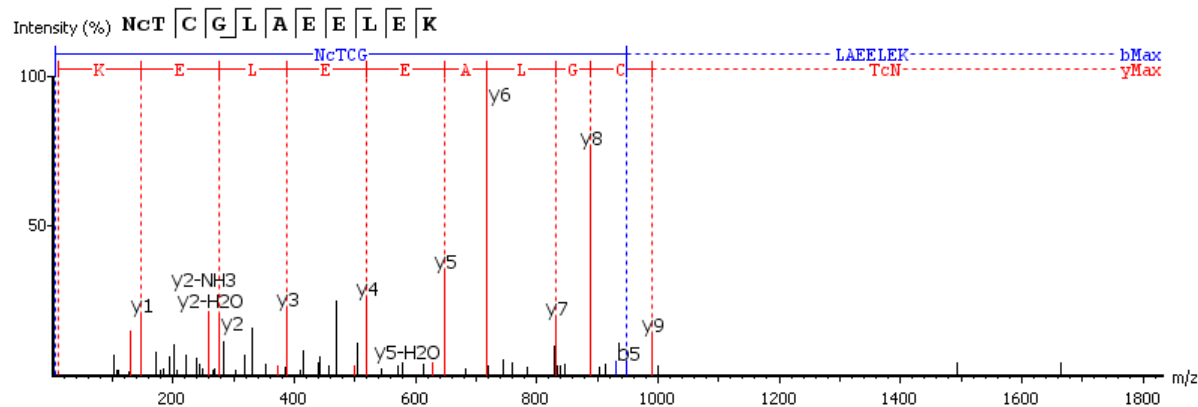
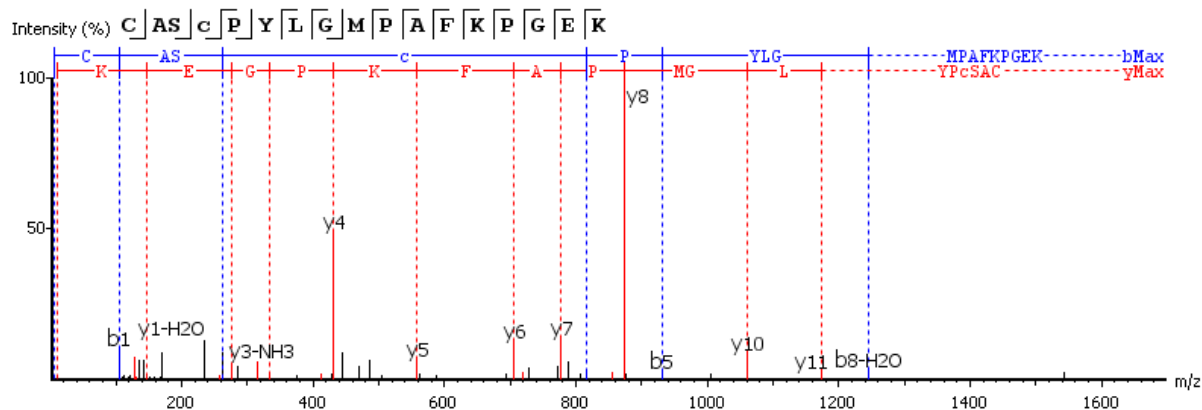
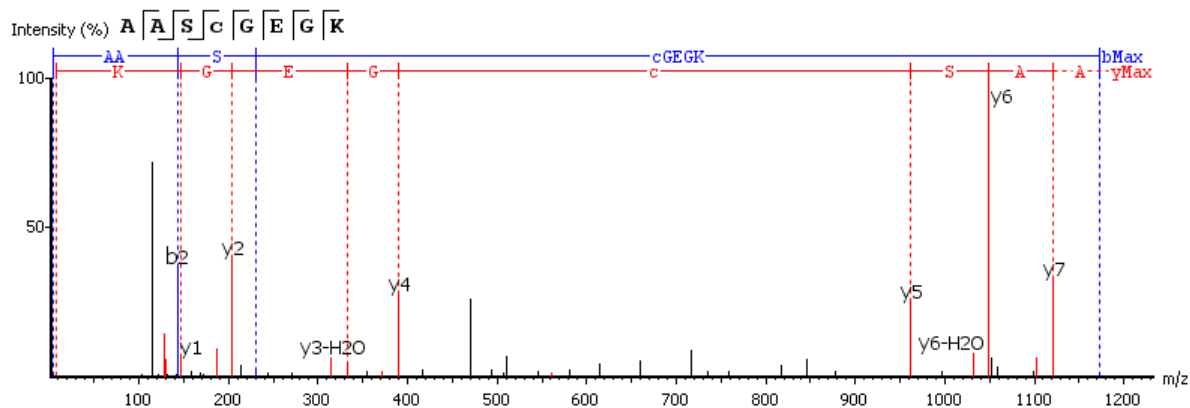
Supplementary Figure 9. CellTiter Glo analysis of cell viability and immunoblot analysis of CIAPIN1 knockdown efficiency following transfection of KMS11 cells with siRNA (CIAPIN1), Scramble or mock control.

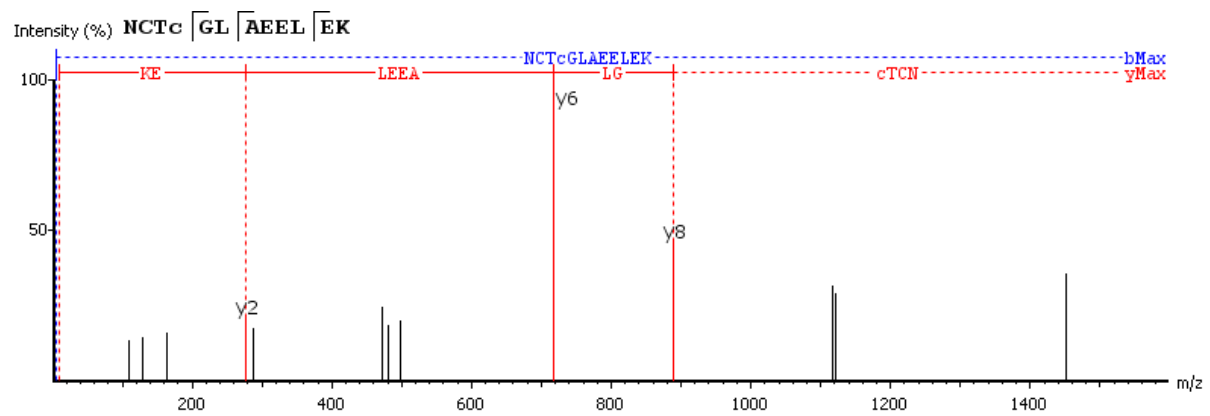


Supplementary Figure 10. (A) Coomassie staining of recombinant CIAPIN1 following incubation with indicated molar equivalent of VLX1570 or DMSO control. (B) ES+ of recombinant VLX1570 bound to CIAPIN1. (C) Cysteine mapping of VLX1570 reveals 7 out of a possible 10 cysteine sites on CIAPIN1 are modified. Peptide coverage is 96%.

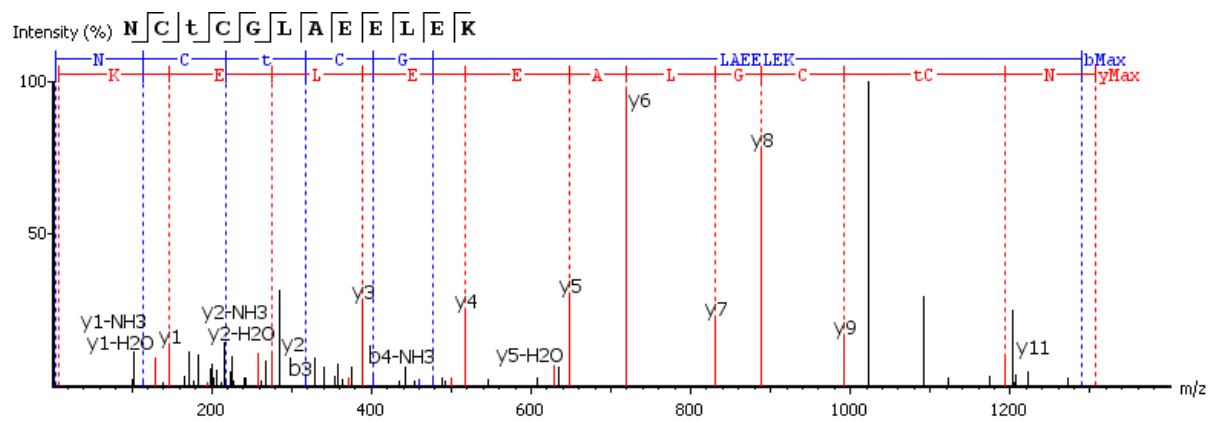
Supplementary Figure 11. Assigned spectra of VLX1570 modified peptides. Lower case represents a modified amino acid.





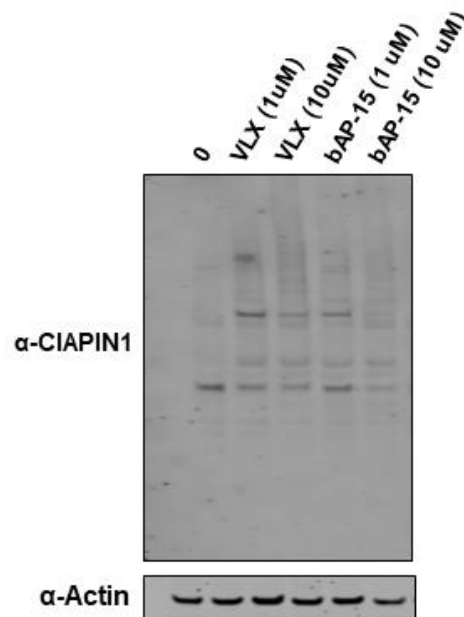


Unmodified Peptide comparison: (retaining disulfide bond)



Supplementary Table 2. VLX1570-modified peptides identified by PEAKs analysis. Mass changes due to VLX1570 (+469.11), oxidation (+15.99) and disulfide bond (-2.02) formation are indicated. RT = retention time

Peptide Sequence	-10LogP	Mass	ppm	m/z	RT
LC(+469.11)SALTLSGLVEVK	74.76	1900.91	-0.6	951.4615	78.05
SACGNC(+469.11)YLGDAFR	69.08	1844.674	0.1	923.3443	74.62
SAC(+469.11)GNCYLGDAFR	66.97	1844.674	-0.3	923.3439	70.4
AASC(+469.11)GEGK	63.57	1190.416	0.3	596.2152	57.64
CASC(+469.11)PYLGMPAFKPGEK	60.5	2266.934	0.9	756.6526	63.21
NC(+469.11)TCGLAEELEK	43.58	1777.678	-0.2	889.8461	67.51
SACGNCYLGDAFRCASC(+469.11)PYLGM(+15.99)PAFKPGEK	33.63	3640.483	1.1	729.1047	56.76
NCTC(+469.11)GLAEELEK	32.71	1777.678	1.2	889.8473	68.89
NCT(-2.02)CGLAEELEK	56.56	1306.553	0.3	654.2841	41.46

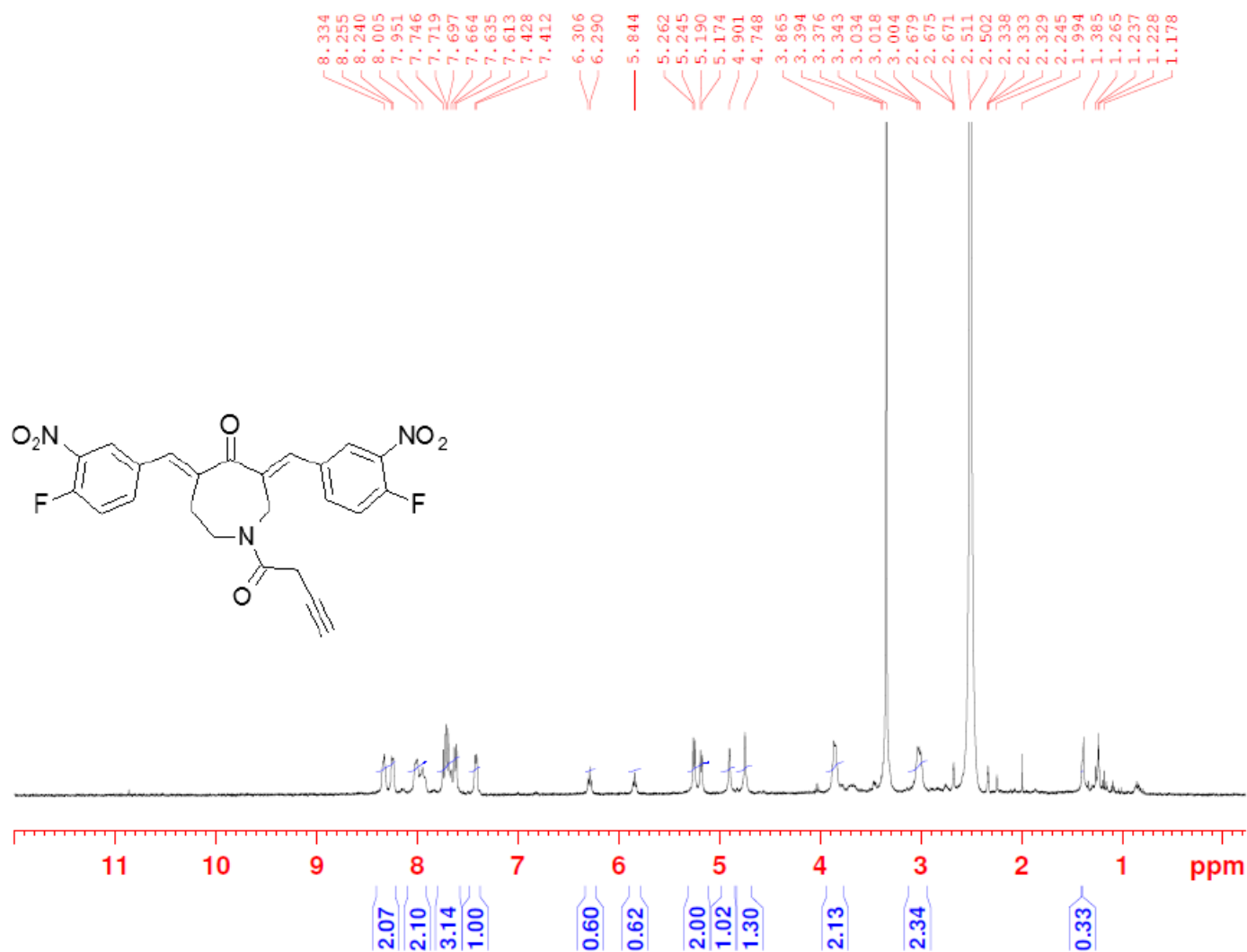


Supplementary Figure 12. Immunoblot analysis of CIAPIN1 following incubation with indicated concentrations of VLX1570 or b-AP15 for 6 hours demonstrated depletion of soluble CIAPIN1.

References

1. Heal, W. P.; Jovanovic, B.; Bessin, S.; Wright, M. H.; Magee, A. I.; Tate, E. W., Bioorthogonal chemical tagging of protein cholesterylation in living cells. *Chem Commun (Camb)* **2011**, 47 (14), 4081-3.
2. Borodovsky, A.; Ovaa, H.; Kolli, N.; Gan-Erdene, T.; Wilkinson, K. D.; Ploegh, H. L.; Kessler, B. M., Chemistry-based functional proteomics reveals novel members of the deubiquitinating enzyme family. *Chem Biol* **2002**, 9 (10), 1149-59.
3. Altun, M.; Kramer, H. B.; Willems, L. I.; McDermott, J. L.; Leach, C. A.; Goldenberg, S. J.; Kumar, K. G.; Konietzny, R.; Fischer, R.; Kogan, E.; Mackeen, M. M.; McGouran, J.; Khoronenkova, S. V.; Parsons, J. L.; Dianov, G. L.; Nicholson, B.; Kessler, B. M., Activity-based chemical proteomics accelerates inhibitor development for deubiquitylating enzymes. *Chemistry & biology* **2011**, 18 (11), 1401-12.
4. Ward, J. A.; McLellan, L.; Stockley, M.; Gibson, K. R.; Whitlock, G. A.; Knights, C.; Harrigan, J. A.; Jacq, X.; Tate, E. W., Quantitative Chemical Proteomic Profiling of Ubiquitin Specific Proteases in Intact Cancer Cells. *ACS Chem Biol* **2016**, 11 (12), 3268-3272.
5. Gasteiger, E.; Gattiker, A.; Hoogland, C.; Ivanyi, I.; Appel, R. D.; Bairoch, A., ExPASy: The proteomics server for in-depth protein knowledge and analysis. *Nucleic Acids Res* **2003**, 31 (13), 3784-8.
6. Ma, B.; Zhang, K.; Hendrie, C.; Liang, C.; Li, M.; Doherty-Kirby, A.; Lajoie, G., PEAKS: powerful software for peptide de novo sequencing by tandem mass spectrometry. *Rapid Commun Mass Spectrom* **2003**, 17 (20), 2337-42.

NMR Spectra of Compound 1



VLX_Supporting information_Submission.pdf (1.24 MiB)

[view on ChemRxiv](#) • [download file](#)

Other files

Supporting Dataset 1.xlsx (110.48 KiB)

[view on ChemRxiv](#) • [download file](#)
